This manuscript was accepted by J. Chem. Phys. Click here to see the version of record.

Molecular origin of aging of pure Se glass: Growth of inter-chain structural correlations, network compaction and partial ordering

S. Dash,[1, a)] P. Chen,[1, b)] and P. Boolchand[1]

Department of Electrical Engineering and Computing Systems,
Solid State Physics and Electronic Materials Laboratory,
University of Cincinnati,
Cincinnati, OH 45221

(Dated: 10 April 2017)

Glass transition width W of pure Se narrows from 7.1(3)° C to 1.5(2)° C and the non-reversing enthalpy of relaxation (ΔH_{nr}) at T_g increases from 0.23(5) cal/gm to 0.90(5) cal/gm upon room temperature aging for 4 months in the dark as examined in Modulated-DSC at low scan rates. In Raman scattering, such aging leads the A1 mode of Se_n-chains (near 250 cm^{-1}) to narrow by 26% and its scattering strength to decrease as the strength of modes of correlated chains (near 235 cm^{-1}) and of Se_8 rings (near 264 cm^{-1}) systematically grow. These calorimetric and Raman scattering results are consistent with the "molecular" chains of Se_n, predominant in the fresh glass, reconstructing with each other to compact and partially order the network. Consequences of the of aging induced reconstruction of the long super-flexible and uncorrelated Se_n-chains are also manifested upon alloying up to 4 mole% of Ge as revealed by a qualitative narrowing (by 25%) of the Raman vibrational mode of the Corner-sharing GeSe4 tetrahedra, and a blue-shift of the said mode by nearly 1 cm^{-1} in 194 cm^{-1}. But, at higher Ge content ($x > 6\%$) as the length of Se_n Chain-segments across Ge crosslinks decreases qualitatively ($\langle n \rangle < 8$), these aging induced chain-reconstruction effects are suppressed. The width of T_g increases beyond 15°C in binary Ge_xSe_{100-x} glasses as $x > 10\%$ to acquire values observed earlier as alloying concentration approaches 20% and networks become spontaneously rigid.

[a)]Present Address: Lam Research Corporation, CA 94538

[b)]Present Address: 105 Verisa Dr., Clarksville, TN 37043

This manuscript was accepted by J. Chem. Phys. Click here to see the version of record.

I. INTRODUCTION

In its elemental form, Selenium is perhaps the only material known that readily forms a bulk glass. Selenium based glasses have been subject to extensive research owing to their high glass forming ability which in turn has paved way for several attractive applications. Amorphous selenium has been commercially exploited in electron photography by Xerox Corp.[1,2] and has also found applications in large area, flat-panel detector for digital radiology[3]. More recently, selenium based chalcogenide materials are being explored for potential applications in the next generation 3D phase change memory devices. Some of the other notable applications are the use of these materials as a photoresist in FIB lithography[4], CD compatible erasable disk, and low-loss IR transmitting devices[5].

Se exists in three allotropic forms, a trigonal form comprising of helical chains, and two monoclinic forms composed of Se_8 monomers. The bulk glass is believed to be composed largely of uncorrelated Se_n-chains with some fraction of Se_8 monomers, although the fraction of these molecular structures present in Se glass has been widely debated[6]. In each instance, since Se is 2-fold coordinated,$(r = 2)$ one expects the Se glass network within Rigidity Theory to be a textbook example of a flexible network. In a covalent solid, bond-stretching forces between nearest neighbors and bond-bending-forces between next-nearest neighbors serve as atomic constraints. When the total count of constraints/atom, nc, equals the dimensionality (n_d) of a network, networks are viewed as isostatically rigid $(n_c = n_d)$. Those with $n_c < 3$ are flexible, while those with $n_c > 3$ stressed rigid. For an atom that is 2-fold coordinated, there is one bond-stretching $(r/2 = 1)$ and one bond-bending $(2r-3 = 1)$ constraint, leading $n_c = (5r/2 - 3) = 2$ constraints/atom[7,8]. Given that both chains and rings are embedded in a 3D structure, $(n_d = 3)$ one expects, 1 floppy mode (F) per atom,

$$F = n_d - n_c = 1 \tag{1}$$

to exist[9], or $1/3^{rd}$ of the vibrational excitations to be floppy. Inelastic neutron scattering measurements[10], indeed, show that in the vibrational density of states, $1/3^{rd}$ of the scattering strength resides in a low frequency mode centered near 5 meV or 40 cm^{-1}. This mode is viewed as the floppy mode predicted by Rigidity Theory, and its frequency upshift from a zero value to a finite frequency (5 meV) is attributed to the presence of inter-chain non-bonding interactions that effectively stabilizes the glass or the crystalline solid.

This manuscript was accepted by J. Chem. Phys. Click here to see the version of record.

Numerous analytical characterization techniques like inelastic neutron scattering[10–15], Raman and IR reflectance[16–24], inelastic X-ray scattering[25], X-ray absorption fine structure[26–29], Mössbauer spectroscopy[30], NMR[31] and DSC[32–37] have been employed to elucidate the nature of structure and excitation in Se glass. By the early 1970s one had broadly recognized from DSC experiments, that the glass transition temperature is close to 45°C, and is characterized by a heat flow curve having a step like feature superimposed by an overshoot which becomes significant upon aging. The overshoot, which represents the enthalpy of relaxation, increases[32,33] over tens of hours upon aging at 23°C in the dark. Enthalpy of relaxation of Se glass also increases by sub-band gap irradiation[38], and for that reason all work related to aging of Se glass reported here was carried out in dark.

In the present work, we have used Modulated DSC to examine the nature of glass transition in elemental glassy selenium upon room temperature aging as a function of waiting time (t_w) in the 0-8 months range. At higher $t_w > 8$ months, onset of nucleation of crystalline fragments is observed in both XRD and Raman scattering experiments. The use of low scan rates (of 3°C/min and lower) in MDSC compared to DSC (10°C/min) has permitted the observation of a rather dramatic narrowing, by almost a factor of 5, in the width W of the glass transition with a concomitant increase by nearly 4-folds in the enthalpy of relaxation at T_g upon RT aging for 4 months. These findings, as we illustrate in the present work, provides the clearest evidence for existence of a growth in *inter-chain structural correlations* of the long super-flexible Se_n-chains as a part of the aging process in pure Se.

We have also examined how the aging effect of polymeric Se_n-chains is altered if their lengths is reduced qualitatively by investigating binary Ge_xSe_{100-x} glasses containing a few mole % of Ge. In pure Se, polymeric Se_n chain length, although widely debated, is generally estimated[6] to exceed 250 atoms at T = 225°C. By alloying 6 mole % of Ge, the average chain length between Ge crosslinks reduces to $\langle n \rangle = 8$ Se atoms. Results demonstrate that the inter-chain structural reconstruction observed in the long chains of pure Se is now qualitatively suppressed in the short ones. At higher Ge concentrations, $10\% < x < 20\%$, the length of the Se_npolymeric chains $\langle n \rangle$' reduces further to the $4 < \langle n \rangle < 2$ range, and a new mechanism of aging is manifested in these glasses. At these higher Ge concentrations, the glass network is better viewed to be composed of largely rigid Cornet-Sharing (CS) and Edge-Sharing (ES) tetrahedral units that are linked by the short but flexible polymeric Se_n fragments. Now, these fragments serve to relieve stress between the rigid tetrahedral units

aging occurs. The resulting increase in the enthalpy of relaxation steadily decreases as x approaches the rigidity transition[39] near $x = 20\%$. Thus, the present work suggests two distinct mechanisms contributing to aging in the present Se-rich glasses: in the low x regime, $0 < x < 10\%$, growth of interchain (secondary) interactions, while at higher x, in the $10\% < x < 20\%$, regime, the short but flexible Se_n chain-segments reconstructing with the near isostatically rigid CS and ES tetrahedral cross-links to globally minimize stress.

A new feature to emerge from our compositional studies on Ge_xSe_{100-x} glassy alloys is the existence of a topological threshold near $x = 3\%$ of Ge, which corresponds to a mean coordination number $\bar{r} = 2\times(1+x) = 2.06$. At this composition, the increase of T_g as a consequence of aging, shows a maximum and we identify it with the decoupling of Se_8 monomers from the backbone.

We present the Modulated DSC and Raman scattering results on pure Se and Se-rich ($x < 10\%$) binary Ge_xSe_{100-x} glasses in section II. This is followed by section III in which we discuss mechanisms of aging of the present Ge-Se glasses. The principal conclusions are summarized in section IV.

II. EXPERIMENTAL

A. Synthesis of pure Se and binary Ge_xSe_{100-x} glasses.

Bulk Ge_xSe_{100-x} binary glasses were synthesized using 99.999% elemental lumps of Ge from Strem Chemicals and Se from Alfa Aesar. Batch sizes were kept at 1 gram. The starting materials in lump form (2-3 mm in diameter) were encapsulated in evacuated (2×10^{-7}Torr) quartz tubes using a Hydrogen-Oxygen torch. Prior to use, the 5mm ID and 7mm OD quartz tube were held in a vacuum oven at 80°C for 24 hours. The sealed precursors were held in a vertical position and reacted in a T-programmable furnace. Pure Se melts were equilibriated at 350°C for 24 hours, and then water quenched. The binary alloy glasses were reacted at 950°C typically for a week[39–41] and then water quenched from 50°C above the liquidus. The alloy glasses were subjected to FT-Raman profiling to ascertain their homogeneity[42]. Once synthesized, these bulk glasses were handled in a glove box "Vacuum Atmospheres model HE-493/MO-5"[43] purged with dry N2 gas with a rel. humidity less than 10^{-3}%. For the FT profiling experiments, Raman spectra were acquired at 8 equidistant locations along

FIG. 1. Profiled FT- Raman spectrum of a Ge_xSe_{100-x} glass , at $x = 4\%$ showing superposition of 8 lineshapes taken along a 20 mm length of the melt column encased in a quartz tube. The identical nature of the observed spectra at different locations confirms homogeneity of the bulk glass. The estimated variation in the stoichiometry in the batch globally is less than 0.25%. Also see ref. of Bhosle et al.[42] CM: Se_n Chain Mode; CS: Corner Sharing Ge(Se1/2)4 tetrahedra; ES: Edge Sharing Ge(Se1/2)4 tetrahedra. See Table II for mode assignments.

a 1 inch long column of the quenched melt contained in an evacuated quartz tube. For all glass compositions in the Ge-Se binary synthesized in the present work, the FT-Raman profiling experiments revealed the melts/glasses to be homogeneous. Fig. 1 shows a typical FT-Raman profiled scan at $x = 4$ %. Dilute alloys of Se with traces of Ge not reacted for sufficient time will lead to bimodal glass transitions[44,45]. For all glasses investigated in the present work, both in the fresh and aged state, we observed only unimodal glass transition temperatures. Next we provide detailed calorimetric characterization of our glasses.

B. Modulated DSC

A model 2920 MDSC from TA instruments Inc., was used to examine the nature of glass transitions. Typically, a 10-15 mg platelet of a glass specimen was sealed in hermetically sealed Al pans. The Al pans and lids were dried overnight in a vacuum oven prior to their use to eliminate any possible contamination from moisture. Once sealed, the glass samples were clearly not subject to either light exposure or the laboratory ambient environment during the course of the aging experiments. All water-quenched glass samples were rejuvenated by heating to T_g and cooled back to RT at 3°C/min to give them the same thermal history. All MDSC scans were undertaken at a modulation time of 100 seconds, modulation amplitude of 1°C and a scan rate of typically 3 °C/min. The enthalpy of relaxation deduced from the non-reversing heat flow was corrected for the finite modulation frequency by subtracting the exotherm observed in the cooling cycle from the endotherm measured in the heating cycle. The frequency corrected enthalpy of relaxation is then independent of the actual modulation frequency used. These details of the MDSC method have been described elsewhere[39,40,42,46–49].

Fig. 2 (b) and (a)shows DSC scans of a fresh (rejuvenated, $t_w = 0$) and a 4 month aged ($t_w = 4$m) glass at RT respectively. The glass transition endotherm overshoot peak height increased nearly fourfolds; from 0.010 cal/gm/sec to 0.040 cal/gm/sec upon aging. The peak of the T_g endotherm is also found to be shifted from 45.4°C to 52.5°C. We will show that the shift in T_g endotherm is purely a kinetic effect that results because of the 10°C/min scan rate used. In these DSC experiments it is difficult to reliably ascertain the enthalpy of relaxation. Generally, one resorts to deconvolution procedure where[50] the total heat flow is considered to be a superposition of a step in the specific heat jump and an assumed Gaussian like enthalpy of relaxation.

FIG. 2. DSC scan of (a) an aged (tw = 4 m) and (b) a fresh (t_w =0) *g*-Se. The same *g*-Se sample when examined in MDSC in the (c) aged (t_w = 4 m) and (d) fresh (t_w = 0 m). A narrowing in the width, "W" of T_g occurs by nearly a factor of 5, and a nearly 5-folds increase in the enthalpy of relaxation , ΔH_{nr} occurs. Use of the low scan rates in MDSC suppresses the kinetic effects that dominate the DSC scans, and has permitted observing the aging induced calorimetric effects in Se glass.

FIG. 3. MDSC scan of *g*-Ge_xSe_{100-x} at $x = 4\%$ in (a) fresh ($t_w = 0$ m) and in (b) in the aged (t_w = 8 m) state. At $x = 4\%$ we also observe the same features of a narrowing of T_g and an increased enthalpy of relaxation upon aging at RT in the dark for 8 m as were observed at $x = 0$, in Fig. 2. To observe this narrow width of T_g in the aged sample, a scan rate of 0.3 °C/min was used.

The same Se glass samples were also examined in MDSC experiments. In MDSC, one imposes a sinusoidal temperature variation over the linear T- ramp, and by using FFT, the observed Modulated heat flow can be directly deconvoluted into a "reversing heat flow component" that tracks the modulations, and a non-reversing heat flow component that does not.[39,47,51]. The reversing heat flow term shows a rounded step-like behavior, and its inflexion point serves to define T_g, while the step height is used to define ΔCp, the change in specific heat at T_g. The width of the glass transition, W (T_g^{end} - T_g^{onset}), is deduced uniquely by the separation between T_g^{onset} and T_g^{end} of the step-like variation of the reversing heat flow

signal (Fig. 2 (c)). Furthermore, the non-reversing heat flow term shows a Gaussian-like profile, with the integrated area under the Gaussian providing the enthalpy of relaxation ΔH_{nr} (Fig. 2 (c)). The ΔH_{nr} term is corrected for the finite modulation frequency by scanning up to T_g (heating), and then cooling down to RT as described elsewhere[47,52,53]. Furthermore, the use of *much lower scan rates* in m-DSC (3°C/min or lower) than in DSC (10°C/min) results in no loss in signal because of the phase sensitive lock in detection capability of AC calorimetry. Furthermore, the use of the much lower scan rates in MDSC compared to DSC, suppresses the kinetic shifts in the calorimetric observables; permitting one to connect these data largely to aspects of glass structural chemistry.

Fig. 2 (d) and (c) show MDSC scans of the pure Se glass in the fresh- and 4 month- aged state respectively. In fresh Se, the frequency corrected enthalpy of relaxation, ΔH_{nr} is found to be 0.23 cal/gm, while T_g, its width W, and the jump in the specific heat at T_g, were found to be 40.7(3)°C, 7.1(3)°C, and 0.030(3) cal/gm/°C respectively. In the 4-months aged Se glass, we found that the T_g remained practically unchanged, $T_g = 40.3$°C, but the ΔH_{nr} term increased four-folds to 0.9 cal/gm. But, perhaps the most striking result to emerge from the MDSC results is a 5-folds reduction in the width of the glass transition W, from 7.1(3)°C to 1.5(3)°C. To record such a narrow glass transition, a scan rate of $1/3^{rd}$ °C/min was used. This dramatic reduction in W is totally masked in DSC because of the kinetic effects.

2. *Se-rich glasses*

To understand how these results on pure Se evolve as the base glass is mildly crosslinked by alloying a few mole % of Ge, we undertook aging experiments on binary Ge_xSe_{100-x} glasses at $x < 10\%$. As an example, we provide MDSC scans at $x = 4\%$ in Fig. 3 b in the fresh state. In this Ge alloyed Se glass, we find T_g, W and ΔCp and ΔH_{nr} to be respectively as 62.1°C, 11.9°C, 0.027(3) cal/gm/°C and 0.17 cal/gm. Upon 4-month aging of this glass composition, we find T_g, W, ΔCp and ΔH_{nr} to be respectively 64.3°C, 3.1°C, 0.026(3) cal/gm/°C and 0.71 cal/gm. These calorimetric results on a Se-rich glass ($x = 4\%$) when compared to those on pure Se ($x = 0\%$), show that an aging induced increase in ΔH_{nr} occurs in both cases. The aging induced reduction in W continues with x unabated (Fig. 4(a)), while the aging induced increase of ΔH_{nr} mildly decreases as x increases to 6% (Fig.

4(b)). In sharp contrast to the case of pure Se where T_g remained unchanged upon aging, in the Se-rich glass at $x = 4\%$, T_g of the glass actually increased from 62.1°C to 64.3°C. While the increase in T_g of 2.2°C is small, it is finite and reproducible and forms part of a global trend (Fig. 4c).

FIG. 4. Summary of MDSC results on g-Ge_xSe_{100-x} at low x ($< 6\%$) , displaying the aging effects at $t_w = 4$ m and 8 m; (a) width of glass transition W, (b) the enthalpy of relaxation, ΔH_{nr}, (c) T_g(x), as a function of Ge content x. In (d) the aging induced increase of T_g is found to display a local maximum near $x = 3.0\%$. The topological threshold is identified with decoupling of Se_8 crowns from the glass network in these dilute alloys. See text for details.

The variation in T_g(x) of aged Se-rich glasses (Fig. 4(c)) shows a small but rather systematic increase over that of fresh ones. To highlight the rather special threshold behavior, we have plotted the aging induced increase of T_g ($= T_g^{\text{aged}} - T_g^{\text{fresh}}$) in (Fig. 4(d)), and find the change in T_g to display a local maximum near $x = 3\%$. Furthermore, the aging induced increase of T_g in these Se-rich glasses aged for 8 months also reveals a local maximum near $x = 3\%$. These data unmistakably point towards the existence of a new topological threshold near $x = 3\%$. (Fig. 4(d)),and we discuss it in Section III.

FIG. 5. Aging or waiting time (t_w) induced changes in the MDSC signals observed in pure Se glass: heat flow (top), reversing heat flow (middle) and non-reversing heat flow (bottom). Aging leads the T_g width W (middle) to narrow and the non-reversing enthalpy (ΔH_{nr}) (bottom) to increase at $t_w = 4$ months. T_g deduced from the inflection point of reversing heat flow (middle) remains unchanged at 40.6(5)°C. The peak in the enthalpy of relaxation(shown by arrows) precursive to T_g, however, steadily shifts closer to T_g (bottom) upon such aging.

FIG. 6. Non-linear trends in the non-reversing enthalpy of relaxation (ΔH_{nr}) and the width of T_g (W) as a function of aging time(t_w) in the $0 < t_w < 18$ month range. The former increases while the latter decreases by nearly a factor of 5 upon such aging. The smooth curves are a guide to the eye.

This manuscript was accepted by J. Chem. Phys. Click here to see the version of record.

2. *Aging induced relaxation in T_g: non-reversing heat flow (ΔH_{nr}) and width W in pure Se*

In section IIB1, we noted the power of MDSC in deconvoluting the endothermic heat flow at T_g into a thermally reversing component (ergodic component) that tracks the sinusoidal temperature variations on a linear T-ramp from a thermally non-reversing one (non-ergodic component) that does not. The results on pure Se glass (**Fig. 5**) taken in the fresh ($t_w = 0$) state are compared to those with the aged ones after waiting times t_w = 0.5m, 1m and 4m. In the top panel of **Fig. 5**, we plot the endothermic heat flow near T_g and find it steadily increases with t_w with the peak shifting to higher T with aging. Such a pattern was noted earlier in DSC data on pure Se as well[32,54]. In DSC experiments, the kinetic shifts to higher T were far greater than those observed in MDSC ones because of the higher scan rates (10 °C/min or greater) used compared to those in MDSC (3 °C/min or less). The middle panel of **Fig. 5**, plots the reversing heat flow signal, which displays a rounded step that steadily narrows as t_w increases in the $0 < t_w < 4$m range. Particularly noteworthy is the fact that the T_g-width W, defined as the temperature difference between the end and onset of the step, is found to be 7.50(5)°C in fresh Se glass but it narrows to 1.50(3)°C in the 4m aged glass. Furthermore, the T_g established from the inflection point of the reversing heat flow remains near 40.6(5)°C, and does not change with aging of the glass. This is exactly what is expected given that each Se atom in a polymeric chain has 2 neighbors, i.e., the connectivity as measured by the mean coordination number $\bar{r} = 2$, and it does not change with aging. T_g is a direct measure of the connectivity of a network[55]. The height of the step in the reversing heat flow between the liquid- and the glass-state has permitted extracting the specific heat change between the two states, and gives $\Delta C_p = C_p^{liq} - C_p^{glass}$ to be 28 mcal/(g.°C) and it is found to be nearly independent of t_w. The bottom panel of **Fig. 5** plots the part of the heat flow that does not track the sinusoidal modulations, i.e., the non-reversing heat flow. It provides a direct measure of the enthalpy of relaxation of the glass building as a glass ages. The term when corrected for the finite but small modulation frequency (10^{-2} cps) yields a value that is independent of the modulation frequency[40]. In our glass studies using MDSC over the years we have noted that the peak in the enthalpy of relaxation (bottom panel of Fig. 5) is always precursive to T_g. Comparison of the present results shown in the middle and bottom panels (**Fig. 5**) confirm that view. However, they also show that as the glass

ages the peak in the enthalpy of relaxation not only increases but it also shifts closer to T_g. The increase in ΔH_{nr} , the integrated area in the non-reversing heat flow signal building up with aging implies that the configurational entropy of the aged glass ($\Delta S = \Delta H_{nr}/T_g$) lowers in relation to the fresh glass.

In **Fig. 6**, we provide a global summary of the variation in $W(t_w)$ and the enthalpy of relaxation $\Delta H_{nr}(t_w)$ as a function of waiting time in the range $0 < t_w < 18$ m. As the glass ages in the dark in a dry ambient environment, the ΔH_{nr} term increases nearly 5 folds while W also decreases nearly 5-folds. The smooth lines through the data points are a guide to the eye. These data suggest that as a Se glass ages at 300K, not only does the configurational entropy decreases but also the inter-chain correlations grow ordering the polymeric chain structure and leading the width of the glass transition to narrow, features we will discuss in section III.

C. Raman Scattering

A Thermo-Nicolet NXR FT Raman scattering facility with a Raman microprobe attachment was used to examine glasses using 1064 nm (1.16 eV) radiation from a Nd-YAG Laser to excite the scattering. The band gap of g-Se and the Se-rich glasses examined exceed 2.18(3) eV[56] and, thus the exciting radiation is transparent to the glasses precluding heating and photocrystallization effects[22,57]. In FT-Raman scattering the use of a notch filter suppresses observing low frequency(< 100 cm^{-1}) vibrational excitations precluding probing Boson mode[21] in the present approach. In a typical measurement 100 mW of the exciting radiation was brought to a loose focus (1000 μm spot size) on a sample either contained in a quartz tube or on a platelet supported on the XYZ stage of the microprobe. FT-Raman profiling of the Ge_xSe_{100-x} glasses was performed to insure melts/glasses were homogeneous[42,58,59]

We have examined changes in the Raman vibrational density of states on account RT aging in the dark on pure Se glass at *waiting times in the* $0 < t_w < 18$ m range. Our measurements reveal that once t_w exceeds 8 months,first indications of t-Se crystallization is observed in Raman scattering as well in X-ray diffraction experiments. These results on pure Se will then be followed by those on Se-rich glasses alloyed with a few mole % of Ge.

Vibrational density of states (VDOS) in Pure Se: role of aging.

FT-Raman spectra of a pure Se glass as a function of RT aging in the dark at several waiting times ranging from a fresh glass (t_w= 0) to t_w = 18 months appear in Fig. 7. For comparison we include Raman spectrum of t-Se in Fig. 7. The observed lineshapes at t_w

FIG. 7. Evolution of Raman spectra of *g*-Se as it ages at RT over a waiting time interval of $0 < t_w < 8$ m. In the low frequency domain, the Raman active mode (138 cm^{-1}) seen in g-Se is associated with the E mode of the uncorrelated Se_n-chains. 142 cm^{-1} is assigned to the E mode of helical chains present in t-Se. In the high frequency domain, the modes A(235 cm^{-1}), B(250 cm^{-1}), C(264 cm^{-1}) come from the A1 mode of correlated chains, A1 mode of uncorrelated chians and A1 mode of Se_8 rings present in g-Se. The bimodal Raman active modes seen near 231 cm^{-1} and 237 cm^{-1} come from the E and A1 mode of helical chains present in t-Se. Refer Table II for detailed mode assignments.

=0, 2 months and 8 months are characteristic of a glass, while the one at t_w = 18 months is that of a Se glass sample that has partially crystallized. A measure of the crystallized fraction of the Se glass sample in question was deduced by correlating the Raman scattering results of Fig. 7 with the powder x-ray diffraction results of Fig. 8.

FIG. 8. Powder X-ray diffraction measurements of *g*-Se in fresh state, *g*-Se aged for t_w = 8 m, *g*-Se aged for 18 m, and trigonal Se. RT aging of Se glass in the dark leads to nucleation of t-Se after a waiting time of 8 months.

A perusal of these results suggests that while the glasses at t_w= 0, 2m, show no evidence of any crystallization, the t_w = 8 m sample has the beginnings of a small fraction of t-Se nucleated. At an increased waiting time of tw = 18 m, we estimate from the x-ray diffraction measurements,that 10(2)% of the glass has crystallized into t-Se. The fraction was obtained by determining the integrated area under the Bragg peaks for the t-Se, to those under the broad hallows characterizing *g*-Se structure. We have also estimated the crystallized fraction from Raman scattering given the mode assignment of the two phases are well established (Table II). Specifically, the triad of modes labelled A, B and C in the 200-260 cm^{-1} range[21], and the E mode near 138 cm^{-1} are characteristic features of the glass

(Table II). Specifically the three modes (Fig. 9(b)) observed in the glass respectively are, A: A1 stretch of correlated polymeric Se_n-chains, B: A1 mode of the uncorrelated polymeric Se_n-chains , and C: A1 intra-ring vibration of Se_8 rings. The narrow pair of modes centered near 231 cm^{-1}(E) and 237 cm^{-1} (A1) are optical phonons of the t-Se phase (Table II). Thus, if one views the Raman scattering lineshape of the t_w= 18 m glass as a superposition of *g*-Se and those of t-Se phases, with the former contributing to the triad of modes A,B and C, while the latter the A1 and E modes , we deduced the t-Se fraction as follows. We obtained the scattering strength of relevant modes to extract the ratio of t-Se/(*g*-Se+t-Se), and found the fraction to be 10 (3)%, in reasonable accord with the XRD results.

FIG. 9. Aging induced changes in the broad-band near 250 cm^{-1} in Raman scattering of *g*-Se (Fig. 7) (a) *g*-Se fresh ,t_w = 0, (b) *g*-Se aged to t_w = 8 months. In (c), we show a superposition of the broad-band deconvolution to highlight aging induced changes. The broad-band is deconvoluted in terms a triad of modes to include mode A (240 cm^{-1}) identified with correlated Se-chains; mode B (250 cm^{-1}) identified with uncorrelated Se-chains, and mode C (260 cm^{-1}) identified with Se_8 crowns decoupled from the backbone. Aging leads to growth in the two minority modes A, C at the expense of the majority mode B as shown in (c).

Next we performed a detailed Raman lineshape analysis in the 200-260 cm^{-1} range for the fresh and 8 month aged Se glass. In deconvoluting the observed Raman spectra in terms of the triad of modes, a Voigt lineshape was used with a Gaussian and Lorentzian mix kept fixed at 95 : 5 with no restrictions on mode-centroid, -width and -scattering strength. Fig. 9 displays the observed broad- band deconvoluted as a triad of modes (A, B and C) in the fresh glass (Fig. 9(a)), and in an 8-month aged Se glass (Fig. 9(b)). To better visualize the role of aging, we have superposed in Fig. 9(c), the triad of vibrational modes of the fresh and aged glasses. Three notable trends become transparent from the deconvolution; (i) the scattering strength of the two minority modes A, C grow at the expense of the majority B mode. (ii) The FWHM of the majority mode B decreases conspicuously from 13.8(3) cm^{-1} to 10.2(3) cm^{-1}, i.e. a reduction of nearly 25% in the linewidth (FWHM). (iii) The B mode frequency remains unchanged upon aging, but the A- and C-mode frequency respectively blue-shift and red-shift as the glass ages. We have extracted the chain fraction of Se glass (Fchain)

$$Fchain = [IB + IA]/[IA + IB + IC], \quad (2)$$

Using equation (2), where IA, IB, IC, represent the normalized scattering strengths of the three modes A, B and C. In fresh Se, the fraction Fchain = 77(5) %, while in the aged state Fchain = 65(5) %. The aging induced reduction in the chain-fraction is due to the growth of the Se_8 ring fraction in the glass primarily.

The chain fraction of Se glass in its fresh state was examined by Yannopoulos and Andrikopoulos[60] as a function of temperature using a lineshape deconvolution method similar to the one used by us. Their results showed the fraction to mildly increase with temperature in the 250 K < T < 350K range, with a value of 83% near 300K. Their value compares favorably with our value of 77(5)% at 300K in the present work. In previous Raman scattering results on Se glass structure studies, we are not aware that aging implications of the chain-fraction in Se glass were considered, and these could well have a bearing in the chain/ring fraction of Se glass that has been widely debated in the literature[61–63]. We will comment on the implications of these results in Section III.

FIG. 10. FT-Raman spectra of g-Ge_xSe_{100-x} alloys in the range $0 < x < 10\%$ studied in the fresh state. The growth in scattering strength of the CS-, ES- mode at the expense of CM as x increases signifies cross-linking of the Se chains. Furthermore each of the modes, CS, ES and CM systematically blue shifts as x increases. The inset shows a plot of the CS mode frequency, $\nu_{CS}(x)$, increasing as x increases. These trends show a general stiffening of the network as cross-linking of the Se-chains ensues.

2. Vibrational density of states (VDOS) in Se-rich glasses lightly alloyed with Ge: the role of aging.

Ge as a crosslinker of polymeric Se_n-chains in binary Ge_xSe_{100-x} glasses has been intensively examined[39,40,64,65] at $x > 10\%$, but much less so at low ($x < 10\%$). Fig. 10 shows the observed Raman lineshapes as a function of Ge content in the Se-rich glasses. These spectra are characteristic of glasses in the fresh state.

Several features become transparent in the Raman VDOS; (i) at $x = 0$, we observe a strongly excited *broad-band* centered near 250 cm^{-1} and a weak mode near 138 cm^{-1}(also

FIG. 11. Role of alloying 2% Ge in Se on broad-band near 250 cm^{-1} in Raman spectrum of (a) the fresh glass , $t_w = 0$, and (b) 8m aged glass. In (c), we highlight aging induced changes by a superposition of the broad-band deconvolution. These aging induced changes observed at x =2% are quite similar to those observed at $x = 0\%$ (Fig. 9).

see Fig. 7), (ii) in the binary glasses (x >0) , we observe a mode identified with Corner-Sharing tetrahedra (CS) near 200 cm^{-1} which steadily blue shifts with increased Ge content 'x'. The latter feature is better seen in the inset of Fig. 10, which shows a plot of the CS mode frequency, νCS(x) as a function of glass composition in the Se-rich phase (iii) In the binary glasses, a vibrational mode near 217 cm^{-1} identified with Edge-Sharing tetrahedral (ES) units is observed, and the scattering strength of the mode steadily increases as the mode frequency blue-shifts with increasing x. (iv) The broad Se- chain band near 250 cm^{-1} ,observed in all the glasses, is found to also steadily blue-shift as x increases.

FIG. 12. Aging induced changes in the FWHM of the majority mode B near 250 cm^{-1} in Raman spectra of g-Ge_xSe_{100-x} alloys in the $0 < x < 10\%$ range. Note that x increases to 10%, the aging induced narrowing of the mode decreases with x and then vanishes as x increases to 10%.

How does the presence of alloying a few mole % of Ge in g-Se alter the aging behavior of the glass? Fig. 11 (a),(b), show Raman scattering results at $x = 2\%$ alloy composition in the fresh glass and in the 8 month aged glass. Upon aging, significant changes are manifested in the observed lineshape that can be observed in Fig. 11 (c) wherein we compare the observed Raman lineshapes of the aged glass with the fresh one. We note that there is a rather striking narrowing of the main mode B upon aging of the glass from ΓB = 12.6 cm^{-1} in the fresh state to ΓB = 9.0 cm^{-1}in the aged state, which represents a 24% reduction in the FWHM. The feature of narrowing of mode B noted earlier continues at higher x (6 %)(Fig. 12) but then vanishes as x increases to 10%.

FIG. 13. Aging induced changes in Raman spectrum of g-Ge_xSe_{100-x} at $x = 2\%$. The CS mode frequency near 200 cm^{-1} blue-shifts and a 25% reduction in its FWHM (see inset) occurs as the glass is aged for t_w = 8 months. Changes in the features of the broad-band mode near 250 cm^{-1} were elucidated earlier in Fig. 11.

This manuscript was accepted by J. Chem. Phys. Click here to see the version of record.

FIG. 14. Aging induced changes in (a) FWHM and (b) frequency of the CS mode from the Raman spectra of glasses in the $0 < x < 10\%$ range. Note that the FWHM reduction continues unabated with x, but the blue-shift decreases with x and then vanishes at $x \rightarrow 10$ upon aging.

FIG. 15. Compositional trends in the scattering strength of (a) the A mode (correlated chains)(b) the B-mode (uncorrelated chains) and (c) the C-mode (Se_8 crowns) upon aging in g-Ge_xSe_{100-x} alloys in the $0 < x < 10\%$ range. The trends show that the minority modes (A, C) grow at the expense of the majority mode (B).

Another significant aging related result at $x = 2\%$ is the rather striking narrowing of the CS mode (Fig. 13) which is clearly displayed in the observed lineshape (see inset of Fig. 13). The result is not peculiar to the $x = 2\%$ composition but persists at higher x as illustrated in Fig. 14 (a). The narrowing of the CS mode is apparently accompanied by a blue-shift of the CS mode Fig. 14(b), providing a clear indication that the rigid Ge cross-links of the long and flexible polymeric Se_n-chains of the glass locally relax and stiffen upon aging. As x increases to 10%, the mode frequency upshift saturates as the length of the Se_n chain segments shortens to $\bar{\mathbf{r}} \simeq 4$ as discussed later in Section III F. Concomitantly, one also observes the E chain mode near 138 cm^{-1} upon aging to blue-shift (Fig. 7), and the Se_n chain mode A to increase in scattering strength giving clear indication that aging promotes polymeric Se_n-chains to become more correlated, as inter-chain interactions grow and the glass network compacts.

We have systematically examined aging effects in Se-rich glasses in the $0 < x < 10\%$ range and a summary of the mode scattering strengths variation is provided in Fig. 15. Our results show the fractional scattering strength increase of mode C (Se_8 rings) (see Fig. 15 (c))upon aging is the largest at $x = 0\%$ but it steadily decreases to vanish as x increases to 10%. In pure Se ($x = 0$), the long polymeric Se_n-chains (mode B) readily transform to Se_8 rings(mode C) and to correlated chains (mode A) upon aging. But such aging induced transformation is qualitatively arrested as the Se_n chain length shortens upon alloying a few mole % of Ge as revealed by the results of Fig. 15.

FIG. 16. Quasi-octahedral coordination of Se in t-Se taken from the work of R. Martin et. al, Reprinted figure with permission from R. Martin and G. Lucovsky, Phys. Rev. B **13**, 1383 (1976), Copyright (1976) by the American Physical Society. The solid lines represent the primary bonding interactions while the colored dashed lines represent the non-bonding interactions with the next nearest neighbors in adjacent Se chains. Here, r is the nearest neighbor distance and R is the next nearest neighbor distance.

III. DISCUSSION

To gain a basic understanding of the structural aspects of aging of Se- glass and Se-rich glasses it is useful to visit the *continuous scale of chemical bonding* of the chain structure of the chalcogens (S, Se, Te) that was introduced by R. Martin et. al[66] in context with metal-insulator transition studies many years back. They found that the ratio (R/r) Fig. 16 of the inter-chain (R) to intra-chain bond length (r) systematically decreases in the sequence, o-S, t-Se, t-Te and cubic Po (Table I). The steady reduction of R/r from t-Se to the more conducting t-Te, and finally to the metallic and cubic Po leads to the equalization of the inter-chain (secondary) interactions with the intra-chain (primary) ones resulting in a insulator to metal transition as one goes down the VIth column of the Periodic table.

In *section A*, we review the *primary bonding* and *secondary non-bonding* interactions that have proved to be fundamental in understanding the structure of polymeric chains of t-Se[66], and of Se glass as well, as we discuss here. These structure related effects in the elemental chalcogens were elegantly probed by Nuclear Quadrupolar Interactions using ^{125}Te and ^{129}I Mössbauer spectroscopy (*Section B*) several years ago and have been pivotal in understanding aspects of chain structure of the Chalcogens. Results of Raman scattering (*Section C*) and Modulated DSC (*section D*) have been insightful in probing aging results that can be traced to the evolution of the secondary interactions in pure Se. In section E, we discuss the aging behavior of the glass transition width W in Ge_xSe_{100-x} glasses in the $0 < x <$20% range which brings out the exceptional nature of the narrowing of W in the super-flexible range, $0< x <$6%. In *Section F*, we discuss for the first time a maximum in aging induced change of T_g in Ge-Se glasses that can be understood in terms of network topology. In *Section G*, we compare present aging results with earlier work. Finally, we conclude with *section H* which puts the present work on the super-flexible Se-and Se-rich

glasses in context with the three known elastic phases of the Ge-Se binary glasses[67].

A. Continuous scales of primary and secondary bonding in elemental chalcolgens

Se in its valence shell has an electronic configuration of $4s^2 4p^4$. Trigonal (t)-Selenium is composed[68] of helical chains running along the c-axis, with corresponding atoms in various chains forming a hexagonal structure (Fig. 16). Two of the p valence electrons with some s orbital hybridization enter into sigma bonds with its two nearest–neighbors (nn) forming intra-chain (covalent) bonds, the *primary interaction*. The primary bond length "r" = 2.373 Å, is close to $2r_c = 2.35$ Å, i.e., twice the covalent radius (r_c) of Se. The s hybridization leads to the opening the Se-Se-Se bond angle[66] from 90° to 103.1°. The remaining two p electrons *(labelled τ in ref. 56)* form non-bonding interactions with two nearest-neighbors (Fig. 16) in adjacent chains. A second interaction primarily of "s" character (*labelled ρ in ref. 56*) form non-bonding interactions with two other Se atoms in adjacent chains. These 4 non-bonding interactions with 3 adjacent chains define the "*secondary interactions*" between the helical chain structure of Se and Te. These secondary interactions are characterized by a bond-length R of 3.46 Å, which is greater than twice the covalent radius of Se (2.35 Å), but less than twice the van der Waals radius ($2r_v$= 4.02 Å) of Se. It led to the suggestion[66] that that these *secondary interactions* are mediated by a mix of covalent and Van der Waals interactions. It is the presence of these secondary interactions that render chains to be helical[69] in nature, a result that drives chains closer together to compact in the t-Se crystalline structure. In t-Te, the secondary interaction become comparable to the primary ones, and one finds the distortion of the octahedral coordination decreases significantly as evidenced by the ^{125}Te Quadrupole interaction in t-Te compared to t-Se as discussed below. In Polonium the primary and secondary interaction equalize and the crystal structure becomes cubic.

A persusal of Table I also illustrates that the ratio R/r in the three polymorphs of Se display an interesting trend- it is the largest for *g*-Se, and the least for t-Se with the case of m-Se in between. These data unambiguously demonstrate that the polymeric Se_n-chains in *g*-Se are more decoupled or molecular, and therefore more structurally disordered versions of those formed in t-Se. *This is precisely what one would have expected based on Phillips[7] criteria for glass formation, viz, the primary bonding interactions serve as constraints remaining intact*

while the weaker secondary non-bonding ones will be partially broken upon glass formation, thus driving the chains to be partially decoupled. The idea is fully consistent with the Se coordination number of 2 for Se glass, as independently confirmed by the scattering strength of the Floppy mode observed in inelastic neutron scattering measurements[10]. The conversion of the "compacted" t-Se chains into the "partially decoupled" ones of g-Se is of more than passing interest. *Aging of g-Se is viewed as a sequence of events in time that partially undoes those that occurred upon melt quenching.*The aging process apparently leads to growth of *secondary interactions* that are observed in Raman scattering and Calorimetric results on pure Se, and Se-rich glasses ($x < 10\%$ of Ge). The narrowing of the Raman mode of polymeric Se_n-chains (~ 250 cm^{-1}) and of the width of T_g as the enthalpy of relaxation increases by an order of magnitude upon long term aging are indirect manifestations of growth of structural order; issues that we shall discuss in sections III C and D.

B. ^{125}Te Electric Field Gradients in the elemental Chalcogen hosts (o-S, t-Se, m-Se, g-Se and t-Te) as a probe for secondary interactions between polymeric chains

We have already noted that the coordination of Se in t-Se leads to a *distorted cubic local structure* (Fig. 16). The lack of cubic symmetry about a Se atom in the polymeric chains of t-Se leads to the existence of a non-vanishing Electric-Field Gradient[70], which, in principle, is directly accessible from NQR. Unfortunsately Se does not have a suitable isotope with a finite Quadrupole moment in the nuclear ground state to perform NQR studies. One can use the nuclear excited state in isovalent Te to probe Nuclear Quadrupole Effects using both ^{125}Te absorption and ^{129}I emission Mössbauer spectroscopy[71,72]. In these experiments performed since the early 1970s, ^{125}Te impurity atoms are doped in the chalcogen host of interest (S, Se or Te) and the EFG at the ^{125}Te site measured. In Table I we provide a summary of ^{125}Te Mössbauer spectroscopy results on g-Se, t-Se, m-Se, o-S and t-Te.

The steadily increasing ^{125}Te nuclear quadrupole splitting (QS) from t-Te to o-S (Table I) as a function of the increasing R/r ratio underscores that "chain decoupling" leads to increased distortion of the Te coordination from cubic symmetry, which is directly measured by ^{125}Te Quadrupole splitting parameter in a Mössbauer effect experiment. These results have been independently corroborated by ^{129}I emission Mössbauer spectroscopy[71]. These

TABLE I. Variation of R/r and ^{125}Te Quadrupole Splitting in indicated chalcogen host.

Host	R/r	^{125}Te (Q.S.)	Reference
o-S	1.61	11.93	Boolchand et. al[70]
g-Se	1.60	11.18	Boolchand et. al[73]
m-Se	1.54	11.33	Henneberger et. al[74]
t-Se	1.45	10.37	Boolchand et. al[75]
t-Te	1.21	7.77	Boolchand et. al[75]

TABLE II. Raman vibrational modes in t-Se and g-Se

Mode Frequency (cm^{-1})	Mode Assignment	References
112	Se_8 rings, A1 mode, glass (out of plane, cis-)	Zallen and Lucovsky[62]
138	Se_n chain, E mode, glass	Zallen and Lucovsky[62]
142	Se_n chain, E mode, t-Se	Zalln and Lucovsky[62]
200	A1 (Ge-Se)Corner Sharing mode, glass	Jackson et. al[76]
212	A1 (Ge-Se)Edge Sharing mode, glass	Jackson et. al[76]
231	Se_n-chains, E mode, t-Se	Zallen and Lucovsky[62]
235[a]	(Correlated) Se_n-chains, A1 mode, glass	Zallen and Lucovsky[62]
237	Se_n-chains, A1 mode, t-Se	Zallen and Lucovsky[62]
250[b]	Se_n-chains, A1 mode, glass	Yannopoulos et. al[21]
264[c]	Se_8 rings, glass (in plane, cis-)	Zallen and Lucovsky[62]

[a] Mode A
[b] Mode B
[c] Mode C

local structure measurements using a pair of nuclear probes are persuasive in demonstrating that as the "secondary non-bonding interactions decrease, a decoupling of the polymeric chain network occurs and leads to an increased distortion of the 6-fold coordination around the chalcogen atom.

C. Raman scattering and aging of g-Se

The principal vibrational features in the Raman spectrum of Se glass (Table II) of interest here consist of a triad of modes[21] in the 240-260 cm^{-1} range which is in agreement with the present work; a majority mode (broad band) near 250 cm^{-1} ascribed to uncorrelated Se_n-chains of a glass, and two minority ones, one near 240 cm^{-1} ascribed to correlated Se_n-chains, and another near 260 cm^{-1} ascribed to Se_8 rings that decouple from the chain structure of the glass. The aging experiments were carried over a 18 month period with Se glass samples hermetically sealed in Al pans and lids at 300K. The majority band is identified[62] with the A_1 symmetric breathing mode of uncorrelated Se_n-chains (Fig. 9 3 panels). Upon 8 months aging of a Se glass we find the uncorrelated Se_n chain mode width (FWHM) narrows by about 26% (from 13.5 cm^{-1} to 10.2 cm^{-1}), (Fig. 12) and the integrated intensity of the two minority modes grow about 15% each at the expense of the majority one (Fig. 15). The narrowing of the 250 cm^{-1} mode constitutes evidence for growth of "interchain correlations" promoting structural ordering of the uncorrelated Se_n-chains native to the fresh glass. Aging induced growth in scattering strength of correlated chain mode (240 cm^{-1}) is a feature that is aging related. The correlated chains represent the eventual fate of the uncorrelated Se_n-chains of the glass as three chain segments reconstruct locally to nucleate a t-Se nanocrystal. With increased aging time, one expects, and indeed observes nucleation of t-Se phase in the glass, as the vibrational mode near 237 cm^{-1} grows in scattering strength (Fig. 7). Separately XRD measurements confirm the nucleation of t-Se in bulk Se glass aged for 1.5 years, thus corroborating the aging induced structural changes inferred from Raman scattering.

The growth in scattering strength of the Se_8 ring mode (260 cm^{-1}) is related to the decoupling of the monomer from the uncorrelated Se_n-chains. We have already seen in Fig. 4 that such decoupling leads to an aging induced increase of T_g in Ge-Se glasses.

D. Aging induced narrowing of calorimetric T_g and increase of enthalpy of relaxation ΔH_{nr}

A Se glass sample aged for 4 months at RT, when examined in MDSC at a scan rate of 3°C/min, yields striking results (Fig. 2(c) and 2(d)). One finds the width of T_g of 7.1°C in the fresh sample ($t_w = 0$) narrows spectacularly to 1.5°C in the aged glass ($t_w =$

ing). The T_g deduced from the inflection point of the step are 40.7(5)°C for the fresh and 40.3(5)°C for the aged glass, showing no change of T_g of Se glass upon aging as one would have expected since the connectivity of the backbone continues to remain at 2. The base glass continues to be 2-fold coordinated, in-spite of some Se_8 crowns decoupling from the backbone.The decoupled Se_8 crowns play no role whatsoever in determining the connectivity of the backbone.

The deconvolution of total heat flow into a reversing and a non-reversing heat flow component[47] is of fundamental importance in glass science. *The reversing (non-reversing) part of the heat flow tracks the ergodic (non-ergodic) component of heat flow.* The *non-ergodic* component of heat flow tracks sample history, impurities and the nature of energy landscape as the melt is cooled. Use of the much lower scan rates in m-DSC without loss in signal permits *complete suppression of kinetic shifts*. At 3°C/min scan rate one goes across the 10°C wide T_g event in 200 seconds, and the glass *network can now track the imposed heating schedule*, thus suppressing the kinetic effect, observed in DSC at 10°C/min scan rate.

The narrowing of the T_g-width, W of pure Se from 7.1 °C to 1.5°C and the concomitant increase in enthalpy of relaxation from 0.23 cal/gm to 0.9 cal/gm upon 4 months of RT aging (Fig. 2(c) and (d)) constitutes evidence of growth in *inter-chain structural correlations between the uncorrelated Se_n-chains* of the glass as it ages. The growth of these structural correlations lowers the configuration entropy of the glass backbone. The reduced width in T_g suggests an increased length of an underlying "*structural coherence length*" describing the growth of interchain interactions. Both these calorimetric observable are consistent with the narrowing of the Raman A_1 vibrational mode of the uncorrelated Se_n-chains (Fig. 7 and 9) and the growth of the Se_8 rings (260 cm^{-1} mode) and the correlated Se_n-chains (240 cm^{-1}). We take these calorimetric and Raman vibrational results as signatures of growth of some *chemical order* of the uncorrelated Se_n-chains as these reconstruct with each other. Reverse Monte Carlo study of a 24 hour annealed Se glass at 300K already show Selenium chains moving closer together and the distribution of interchain distances narrowing in relation to the freshly quenched glass. The reconstruction is viewed as adjacent chains locally displacing laterally (normal to the chain axis) to come together and to acquire quasi-helical like structure. Indeed, prolonged aging, for 8 months at 23°C ($T/T_g = 300K/317K = 0.946$), leads to some chains reaching their ultimate fate, i.e. nucleation of t-Se grains in an otherwise glassy matrix, as observed in XRD scan (Fig. 7). The t-Se fraction grows steadily to nearly

This manuscript was accepted by J. Chem. Phys. Click here to see the version of record.

10% volume fraction as the waiting time is increased to 1.5 years as revealed by both XRD and Raman scattering (Fig. 7 and 8).

E. Aging behavior of Se-rich binary Ge_xSe_{100-x} glasses

What would be the role of alloying a few mole% of Ge in a Se-rich glass on the aging behavior? Fortunately, the molecular structure of binary Ge-Se glasses has been intensively examined over the past 3 decades or more in Raman scattering[40,42,59,64,67,77] , Mössbauer spectroscopy[70,78,79], calorimetric measurements[42], neutron scattering measurements[80,81] and MD simulations[82,83]. We discuss these results here and show that Ge alloying of a Se glass rapidly suppresses the striking aging induced structural effects observed in pure Se.

Se glass is largely characterized by uncorrelated Se_n-chains whose average length has been inferred from viscosity measurements to exceed[61,84] 250 atoms. Assuming Ge cross-links the polymeric uncorrelated Se_n-chains in Se glass to form Ge(Se1/2)4 tetrahedra, one can show from statistical counting that the length of Se_n chain segments $\langle n \rangle$ between Ge-crosslinks initially decreases rather rapidly with Ge content 'x' in binary Ge_xSe_{100-x} glass but eventually slows down as shown in Fig. 17. In this simple approach, we only consider corner-sharing tetrahedra, i.e. we exclude edge-sharing tetrahedra. The results show that near $x = 6\%$ Ge, $\langle n \rangle \simeq 8$, and near $x = 20\%$ Ge, $\langle n \rangle \simeq 2$ (Fig. 17)

FIG. 17. A simple statistical counting model shows the average chain length as a function of mean coordination number/composition in Ge_xSe_{100-x} glasses. Typically, chain length is >250 in pure Se, but reduces to 2 atom long in Ge20Se80. An average chain length $\langle n \rangle$ of 8 is expected near x = 6%

Modulated DSC experiments on the binary Ge-Se glasses show glass transition width W upon aging, as in pure Se, to also decrease in the lightly Ge-doped Se glasses.The narrowing of the width W of T_g upon aging is the largest in pure Se, but it steadily decreases as a function of Ge content as shown in Fig. 4(a) .Furthermore, the aging induced increase in the enthalpy of relaxation, $\Delta H_{nr}(x)$ is the largest in pure Se, but it steadily decreases as the Ge content of the binary Ge-Se glasses increases to 6% (Fig. 4(b)). These compositional trends highlight the fact as the length of the polymeric Se_n-chains $\langle n \rangle$ decreases upon Ge alloying, aging induced reconstruction is steadily suppressed.

FIG. 18. Observed FWHM of T_g , W(x) in fresh ($t_w = 0$; open circles) and 4 month aged (t_w = 4m; filled circles) of binary Ge_xSe_{100-x} glasses. The aging induced average fractional reduction in W (0.65), (see equation 3), is remarkably high in the composition range R_1, but it is vanishing small (W $\sim$ 0) in the composition range R_3, with the range R_2 serving as a transition region. R_1 is identified with the super-flexible glass compositions in the present binary.

1. *Super-Flexible regime*

A particularly powerful feature of MDSC as a probe of glass transitions is that it permits a direct measurement of the width (W) of T_g from the reversing heat flow signal as noted earlier in section IIB. We compare in **Fig. 18** the width (W) of T_g of pure Se glass with those of Se-rich binary Ge_xSe_{100-x} glasses in the $0\% < x < 20$ composition range, i.e., the flexible phase[39,85] of these glasses. In the fresh glasses ($t_w = 0$) one finds that W(x) steadily increases from a value of 7.50(5) °C at $x = 0$ (pure Se) to 40(1)°C at $x = 20\%$. The glass network connectivity measured in terms of the mean coordination number, $\bar{r} = 2(1 + x)$ increases linearly with x in the range $2.00 < \bar{r} < 2.40$. These data already suggest that the T_g - width W(x) in the as prepared fresh glasses scales quasi-linearly with the connectivity of the glasses probably because as Ge atoms crosslink the flexible Se_n-chains the glass network backbone becomes mechanically more constrained promoting W. Most revealing however, is the fact that aging induced fractional reduction in W, i.e., $\Delta W/W$, defined as follows:

$$\frac{\Delta W}{W} = \frac{W(t_w = 0) - W(t_w = 4m)}{W(t_w = 0)} \tag{3}$$

although rather high in the range R_1, ($0 < x < 6\%$), actually vanishes at in the $10\% < x < 20$ % composition range, i.e., the range R_3 as shown in **Fig. 18**. The aging induced reduction $\Delta W/W$ is close to 0.80 in pure Se ($x = 0\%$) and near 0.50 at $x = 6\%$. But in the range R_3, $\Delta W/W \approx 0$.

Why do glasses in range R_1 behave so differently from those in range R_3 although both are broadly viewed to be in the flexible elastic phase of the present Ge-Se binary? The average length of the polymeric Se_n-chains in these binary glasses is estimated to decrease **(Fig. 17)** in a highly non-linear fashion from about $\langle n \rangle > 250$[61] at $x = 0$, to nearly 8 at $x = 6\%$. At higher x, particularly in range R_3, changes in $\langle n \rangle$ occur in the $8 < \langle n \rangle < 2$ range, i.e., they are minimal. For the aging induced width W to decrease inter-chain

structural correlations must be promoted. Chains must be long, and each chain laterally surrounded by at least 4 other ones to nucleate elements of intermediate range structure characteristic t-Se (**Fig. 16**).The aging induced promotion of the interchain interactions drives these to become quasi-helical and thus compact the glass as noted earlier. In the range R_1 the polymeric Se_n-chains in the glass are also extremely flexible because $1/3^{rd}$ of the vibrational modes are floppy[86] , i.e., there is the absence of dihedral angle restoring forces of these chains as confirmed earlier from neutron scattering[10,30,87]. At $x > 6\%$, not only do the chains reduce in length but the chain ends become Ge crosslinked, which serve as a barrier for the Se_n-chains to reconstruct, and leads $\Delta W/W$ to vanish at $x \geq 10\%$ (**Fig. 18**). It is for these reasons we believe the range R_1 (**Fig. 18**) is so special and view glassy networks formed in the range R_1 to be super-flexible.

The aging induced growth in structural order of the polymeric Se_n-chains in the super-flexible R_1 range has profound consequences on the vibrational behavior of the $GeSe_4$ CS mode, which not only stiffens **(Fig. 14)** but also narrows **(Fig. 13)** as revealed by Raman scattering results. The actual lineshape observed is reproduced in the inset of Fig. 13. Lineshape analysis shows that the CS mode width $\Gamma = 12.2(3)$ cm^{-1} in the fresh glass, reduces to $\Gamma = 9.2(3)$ cm^{-1} (Fig. 14) in the aged glass, representing a 24.5% reduction. (b) The mode width Γ reduction continues at higher Ge alloying concentrations in the $2 < x < 10\%$ range unabated.(c) However, the *aging induced* blue-shift of the CS mode frequency, which is 0.52% at $x = 2\%$, steadily decreases and then vanishes (Fig. 14) as x increases to 10%. This is a curious result. To understand the implications of the result, one has to recognize that there are two types of network compaction effects taking place: one coming from the aging induced inter-chain reconstruction, and the second from the Ge chemical alloying based compaction[42] as the alloyed network steadily crosslinks and approaches towards isostaticity, i.e., n_c approaches 3 near $x = 20\%$. At low x ($< 6\%$), the chemical alloying induced compaction effect is small, permitting the aging induced network compaction to come into play.

The most prominent aging induced feature in the vibrational density of states of these glasses is the narrowing of the A_1 chain-mode of the uncorrelated Sen chain (Fig. 13 and 14). The FWHM of the 250 cm^{-1} mode narrows by nearly 25% upon 8 month aging in Se glass (Fig. 14). A perusal of the plot of Fig. 14, also shows that as Ge is steadily alloyed in Se, the *aging induced change* in the width of the A_1 chain mode is found to continue

This manuscript was accepted by J. Chem. Phys. Click here to see the version of record.

nificant as x increases to 10% (Fig. 14)

To summarize, in the super-flexible regime , $0\% < x < 6\%$ range, interchain structural correlations grow and , in general, lead to a significant aging induced compaction of the glass. At $x > 6\%$, Ge atoms as cross-linkers of Se_n-chains also serve to compact the alloyed glass network[39,42] but by an entirely different mechanism, viz, increased network connectivity leading to the mechanical constraints/atom, n_c steadily increasing to approach the threshold value of 3 near $x = 20\%$ of Ge. We discuss the issue next.

2. Flexible regime

The second domain of aging is manifested in the flexible range, i.e., $6\% < x < 20\%$ range, where a new microscopic origin of aging emerges. In this composition range the flexible Se_n chain segments become quite short ($2 < \langle n \rangle < 4$) in length, thus growth of inter-chain structural correlations ceases to be the principal relaxation mechanism. However, these short "flexible" chains serve to assist relaxation of the "rigid" chains of tetrahedral units comprising the glass network as it is steadily crosslinked and approaches the percolation of rigidity. And we find that the width Γ of the CS mode in a glass at $x = 10\%$ reduces by almost 25% upon 8 month aging of glasses at RT. The bond-bending (angular force) constraining the Se-Ge-Se bond angle of the CS $GeSe_4$ tetrahedral units will overwhelm the angular force of the Se-Se-Se polymeric Se_n-chains, and drive them to their ideal value of 109.9 °C.

Thus, aging of glasses in the $6\% < x < 20\%$ composition range is driven largely by local rearrangements of the CS and ES tetrahedral units facilitated by the short but still flexible Se_n chain segments. In addition to that, one clearly observes the enthalpy of relaxation to build up upon aging of rejuvenated glasses[39,42].

F. Aging induced increase of T_g in super-flexible glasses ($0 < x < 6\%$): evidence of a new topological threshold near $x = 3\%$.

The glass transition temperature (T_g) variation in binary Ge-Se glasses as a function of Ge content has been widely studied in the field. The observed variation has been quantitatively understood in terms of stochastic agglomeration theory[55], especially at low Ge alloying

content ($x < 15\%$). Here we made a special effort to examine the T_g of the aged glasses and in Fig. 4(c) and (d) we compare the T_g of the fresh and aged glasses in the super-flexible regime ($0 < x < 6\%$). We find T_g of the aged glass to be in general greater than the fresh glass, and the difference T_g^{aged} - T_g^{fresh} to display a maximum near $x = 3\%$. At the outset these differences in T_g can neither be ascribed to quench rate effects, since all melts were cooled from T_g at 3°C/min nor to the kinetic shifts since the scan rates used in these MDSC experiments were kept at 3°C/min or lower.

Raman scattering measurements presented earlier in Fig. 7 and 9 have shown that prolonged aging of pure Se glass at RT leads to the decoupling of Se_8 crowns from the backbone. Specifically we noted that the scattering strength of the 260 cm^{-1} mode grows at the expense of the 250 cm^{-1} mode due to the growth of correlations between the polymeric Se_n-chains upon aging (Fig. 15). These results strongly suggest that the increase of T_g in the $0< x < 3\%$ range is due to an *aging induced decoupling* of Se_8 crowns from the backbone, which leaves the backbone Ge-richer with a higher T_g than the fresh glass. One regards T_g to be a faithful measure of the connectivity of the backbone[55,88]. At $x = 0$, although the aging induced decoupling of Se_8 crowns is at a maximum, a change in T_g brought about by such decoupling does not manifest. On the other hand with a finite concentration of Ge alloyed, the decoupled Se_8 crowns play the role of *increasing the connectivity of the backbone* by increasing its effective Ge-concentration. The increase of T_g upon aging of Se-rich glasses from 4 months to 8 months, (Fig 4(d)) is the result of an increased decoupling of Se_8 rings from the backbone. But at $x > 6\%$, the aging induced increase of T_g vanishes since the average chain-length between Ge crosslinks approaches near $\langle n \rangle = 8$ (Fig. 17). Thus, as x increases in the $3\% < x < 6\%$ range the probability of Se_8 crowns decoupling from the backbone will steadily decrease and actually vanish as x approaches 6%. The presence of Ge additive permits a change in T_g to be detected as Se_8 rings decouple from the backbone. Thus the change in T_g is more easily detected as the Ge content increases. We view the threshold at $x = x_c = 3.0\%$ to be a compromise composition where the T_g enhancement due to segregation of Se_8 crowns is maximized. If Se_8 rings persisted as coupled to the polymeric Se_n-chains as suggested elsewhere[89], there would be no T_g increase.

G. Correlating present work on aging of Se and Se-rich glasses with earlier work

1. *Se_8 fraction in in fresh and aged g-Se*

Our Raman scattering experiments on g-Se reveal that the Se_8 ring to Se_n chain fraction, Fring, in a *fresh glass* is near 23%. A slightly smaller value of 17% for this fraction was deduced[21] from an earlier Raman scattering measurements[21]. In both instances, the fraction was deduced from the broad band near 250 cm^{-1} that was deconvoluted in terms of a triad of modes as discussed earlier. Upon 8 month aging of g-Se at RT in the dark the fraction, Fring increased to 36% (Fig. 9 and 15). Yannopoulos et al.[21] did not investigate aging related changes in the ring-chain equilibrium of g-Se. Topologically, the principal difference between a Se_8 ring and a t-Se chain is that the dihedral angle alternates in sign for a ring (leading to its closure) but remains the same for a chain (leading to its propagation in a quasi-helical fashion). Available structural data on t-Se and α-Se shows that the Se-Se bond length (2.32 Å, 2.373 Å) and the Se-Se-Se bond angle (105.9°, 103.1°) and the dihedral angle (101.0°, 100.6°) for these two structural units(α-Se,t-Se) are quite similar[66]. Furthermore , based on the Raman results on the T-dependence of the ring/chain[60], the activation energy required is 15 meV to convert Se_n-chains into Se_8 rings at RT ($T < T_g$) which is quite small. One can expect at RT (25.9 meV) aging of g-Se to facilely proceed to overcome the steric hindrance from chains to rings. Given the presence of substantial photostructural effects in g-Se[90], it would be useful to use the present Raman scattering approach to quantitatively establish the IR radiation induced ring/chain fraction evolution as a function of light integrated dose. Such information would be particularly useful to better understanding the Se ring fraction results of Brieglieb[61] by chemical dissolution where a substantially higher ring fractions was inferred.

2. *Bimodal T_gs and heterogeneity of Se-rich binary Ge-Se glasses.*

The aging of elemental Se and binary Ge-Se[44] and As-Se glasses has been the subject of several previous reports. Saiter et al.[45] and independently Golovchak et al.[44]examined aging effect in binary Ge-Se glasses. These investigations made use of DSC as a means to measure the enthalpy of relaxation and T_g at a scan rate of 10°C/min. In these experiments there

ing substantial kinetic shifts in the endothermic heat flow that lead to higher T_g and led these authors to completely miss observing the narrowing of the glass transition upon aging at low Ge content that we report here. The bimodal T_gs observed at low Ge contents (2%, 4%, 8%) in binary Ge-Se glasses[44,45,91] most likely are due to glass stoichiometry variation across the batch compositions. In our experiments on homogenized Se-rich binary Ge-Se glasses, we observed only unimodal glass transitions both in fresh and aged glasses. In several recent reports[48,59] we have traced the "slow" kinetics of Ge-Se melt homogenization to be the consequence of the "superstrong behavior" (or low fragility index , m = 16) at intermediate phase melt compositions (20 %$< x <$ 26%), which serves as a diffusive barrier to homogenize melts at *any composition*[48,49,59,92] synthesized in the present binary.

FIG. 19. A topological phase diagram is constructed which displays 2 elastic phase transitions and a nano-scale phase separation[40] near x =31.5%. In the super-flexible regime, different thresholds are identified which dictate the relaxation mechanism in operation.

H. Global Elastic Phase Diagram of Ge-Se binary glass system

Glass/melt homogeneity is precursive to observing the intrinsically sharp rigidity- and stress-transitions respectively near $x = 20\%$ and 26% of Ge as discussed elsewhere[67]. When we combine the present results in the super-flexible and flexible phases with those established earlier in the intermediate phase and the stressed-rigid phase at higher Ge concentration, a global elastic phase diagram of the Ge-Se binary including the various topological phases can be constructed (Fig. 19). In the super-flexible phase aging proceeds by interchain reconstruction and Se_8 rings decoupling. In the flexible plase the short Se_n segments between the Ge-crosslinks serve to relax the network as the enthalpy of relaxation steadily decreases. At the onset of rigidity near $x = 20\%$ the enthalpy of relaxation becomes minuscule and remains so till the onset of stress at $x = 26\%$, when the enthalpy of relaxation increases precipitously with x[39]. At $x > 31.5\%$ of Ge, the bulk glasses begin to partially segregate into Ge-rich and Se-rich regions for which substantial evidenvce has accrued from Calorimetric[39], Raman[42] and Mössbauer effect[93,94] studies. The Nano-scale phase separation (NSPS) transition near 31.5% of Ge leads naturally to the segregation of the stoichiometric glass $GeSe_2$ (x =33.3%) into Se-rich and Ge-rich clusters[93,94].

IV. CONCLUSIONS

Raman scattering and Modulated DSC experiments are undertaken on pure Se and binary Ge_xSe_{100-x} glasses containing up to $x = 10\%$ of Ge. Aging was examined at 23°C with glass samples encapsulated in hermetically sealed Al pans over a waiting time(t_w) in the $0 < t_w <$ 8 months range. Several conclusions can be drawn from the present work. (a) In pure Se, the width of the glass transition $W(t_w)$ narrows spectacularly from 7.1°C to 1.5°C in 4 months, while the non-reversing enthalpy, $\Delta H_{nr}(t_w)$ increases from 0.23 cal/gm to 0.90 cal/gm in the same period. (b) Both calorimetric observables (W, ΔH_{nr}) change by nearly a factor of 5. (c) In Raman scattering, the A1 mode of the uncorrelated chains near 250 cm^{-1} in pure Se narrows by 26% upon aging for 4 months. Features (a), (b) and (c) constitute the thermal (a,b) and optical (c) signatures of "molecular" Se_n-chains of the fresh glass reconstructing with each other to compact and structurally order the glass network. Such reconstruction is mediated by the growth in inter-chain secondary interactions at the expense of intra-chain primary ones and leads to a lowering of the configurational entropy of the relaxed Se glass in relation to the fresh one. (d) In pure Se, an aging induced reduction of about 20% in Raman scattering strength of the A1 mode of "molecular chain" of the fresh glass is observed at the expense of a growth of about 14% in scattering strength of vibrational modes of Se_8 crowns (near 260 cm^{-1}) and a growth of about 6% in the correlated Se_n-chains (237 cm^{-1}) upon an 8 month aging period. Observation (d) shows that decoupling of Se_8 crowns from the fresh glass network is an intrinsic aging induced process that also serves as an entropy sink. (e) In binary Ge_xSe_{100-x} glasses as the Ge content x of glasses increases steadily from 0 to 6 mole%, the aging effects outlined above in features (a), (b), (c) and (d) are each systematically suppressed as the length of the Se_n-chain segments between the Ge-crosslinks decreases and drives the super-flexible network of pure Se glass to become steadily more rigid. (f) Finally, a new topological threshold is observed in binary Ge_xSe_{100-x} glasses near $x = 3\%$ of Ge, where a maximum in the aging induced increase of T_g (ΔT_g = T_g(aged) - T_g(fresh) is observed, whose microscopic origin is traced to the decoupling of Se_8 crowns from the base alloyed glass network. These profound room temperature (23°C) aging effects of pure Se with a T_g (40.5°C) derive from the super-flexible elastic nature of the chain-glass network.

V. ACKNOWLEDGMENTS

We have benefited from discussions Dr. Matthieu Micoulaut, Dr. Kapila Gunasekera, Dr. Sriram Ravindren, Dr. Chad Holbrook, Dr. John Mauro, Siddhesh Bhosle, Aaron Welton and Dr. Caleb McDonald during the course of this work. The present work represents in part the Masters Thesis of S. Dash at University of Cincinnati. This work was supported by NSF grant DMR 08-53957.

REFERENCES

[1]M. R, "Electrophotographic copying apparatus," (1962), uS Patent 3,062,108.

[2]D. Buckley, "Preparation of red amorphous selenium," (1977), uS Patent 4,007,255.

[3]J. Rowlands and S. Kasap, Physics Today **50**, 24 (1997).

[4]T. Gilton, S. Bowes, J. Moore, J. Brooks, and K. Campbell, "Semiconductor processing method using photoresist and an antireflective coating," (2003), uS Patent App. 10,071,425.

[5]J. Lucas, "Chalcohalide glasses," in *Insulating And Semiconducting Glasses*, edited by P. Boolchand (World Scientific, 2000) pp. 691–728.

[6]W. C. Cooper and R. Westbury, "The structure of selenium," in *Selenium*, edited by R. Zhigaro and W. C. Cooper (Van Nostrand Reinhold Company, New York, 1974) pp. 87–147.

[7]J. C. Phillips, Journal of Non-Crystalline Solids **34**, 153 (1979).

[8]J. Phillips, Journal of Non-Crystalline Solids **43**, 37 (1981).

[9]M. F. Thorpe and M. V. Chubynsky, "The intermediate phase and self-organization in network glasses," in *Phase Transitions and Self-organization in Electronic and Molecular Networks*, edited by J. C. Phillips and M. F. Thorpe (Kluwer Academic/Plenum Publishers, 2001) pp. 43–64.

[10]W. A. Kamitakahara, R. L. Cappelletti, P. Boolchand, B. Halfpap, F. Gompf, D. A. Neumann, and H. Mutka, Physical Review B **44**, 94 (1991).

[11]I. Petri, P. S. Salmon, and H. E. Fischer, Physical review letters **84**, 2413 (2000).

[12]F. Gompf, Journal of Physics and Chemistry of Solids **42**, 539 (1981).

[13]W. Phillips, U. Buchenau, N. Nücker, A.-J. Dianoux, and W. Petry, Physical review letters **63**, 2381 (1989).

[14]M. Garcia-Hernandez, F. Bermejo, B. Fåk, J. Martinez, E. Enciso, N. Almarza, and A. Criado, Physical Review B **48**, 149 (1993).

[15]M. Foret, B. Hehlen, G. Taillades, E. Courtens, R. Vacher, H. Casalta, and B. Dorner, Physical review letters **81**, 2100 (1998).

[16]G. Lucovsky, A. Mooradian, W. Taylor, G. Wright, and R. Keezer, Solid State Communications **5**, 113 (1967).

[17]M. Gorman and S. Solin, Solid State Communications **18**, 1401 (1976).

[18]P. Carroll and J. Lannin, Solid State Communications **40**, 81 (1981).

[19]G. Lucovsky and C. Wong, Philosophical Magazine B **52**, 331 (1985).

[20]V. Bogomolov, V. Poborchy, S. Romanov, and S. Shagin, Journal of Physics C: Solid State Physics **18**, L313 (1985).

[21]S. N. Yannopoulos and K. S. Andrikopoulos, The Journal of Chemical Physics **121**, 4747 (2004).

[22]K. A. V. Poborchii V V and K. Tanaka, Appl. Phys. Lett. **74**, 215 (1999).

[23]A. Roy, A. V. Kolobov, and K. Tanaka, Journal of applied physics **83**, 4951 (1998).

[24]V. V. Poborchii, A. V. Kolobov, and K. Tanaka, Applied physics letters **72**, 1167 (1998).

[25]T. Scopigno, R. Di Leonardo, G. Ruocco, A. Baron, S. Tsutsui, F. Bossard, and S. Yannopoulos, Physical review letters **92**, 025503 (2004).

[26]C. Yang, D. Sayers, and M. Paesler, Journal of Non-Crystalline Solids **114**, 67 (1989).

[27]K. Tamura, M. Inui, M. Yao, H. Endo, S. Hosokawa, H. Hoshino, Y. Katayama, and K. Maruyama, Journal of Physics: Condensed Matter **3**, 7495 (1991).

[28]S. De Panfilis and A. Filipponi, EPL (Europhysics Letters) **37**, 397 (1997).

[29]M. Majid, S. Benazeth, C. Souleau, and J. Purans, Physical Review B **58**, 6104 (1998).

[30]P. Boolchand, R. Enzweiler, R. Cappelletti, W. Kamitakahara, Y. Cai, and M. Thorpe, Solid State Ionics **39**, 81 (1990).

[31]W. W. Warren Jr and R. Dupree, Physical Review B **22**, 2257 (1980).

[32]R. B. Stephens, Journal of Non-Crystalline Solids **20**, 75 (1976).

[33]R. Stephens, Journal of Applied Physics **49**, 5855 (1978).

[34]P. Cortes, S. Montserrat, J. Ledru, and J. Saiter, Journal of non-crystalline solids **235**, 522 (1998).

[35]I. Echeverrıa, P. L. Kolek, D. J. Plazek, and S. L. Simon, Journal of non-crystalline solids **324**, 242 (2003).

[36]J. Málek, R. Svoboda, P. Pustková, and P. Čičmanec, Journal of Non-Crystalline Solids **355**, 264 (2009).

[37]J. Hutchinson, Journal of thermal analysis and calorimetry **72**, 619 (2003).

[38]P. Lucas, A. Doraiswamy, and E. A. King, Journal of Non-Crystalline Solids **332**, 35 (2003).

[39]S. Bhosle, K. Gunasekera, P. Boolchand, and M. Micoulaut, International Journal of Applied Glass Science **3**, 205 (2012).

[40]S. Bhosle, K. Gunasekera, P. Boolchand, and M. Micoulaut, International Journal of Applied Glass Science **3**, 189 (2012).

[41]R. Bhageria, K. Gunasekera, P. Boolchand, and M. Micoulaut, Physica Status Solidi B-Basic Solid State Physics **251**, 1322 (2014).

[42]S. Bhosle, K. Gunasekera, P. Chen, P. Boolchand, M. Micoulaut, and C. Massabrio, Solid State Communications **151**, 1851 (2011).

[43]D. I. Novita, P. Boolchand, M. Malki, and M. Micoulaut, Journal of Physics: Condensed Matter **21**, 205106 (2009).

[44]R. Golovchak, A. Kozdras, O. Shpotyuk, S. Kozyukhin, and J.-M. Saiter, Journal of Materials Science **44**, 3962 (2009).

[45]J. M. Saiter, M. Arnoult, and J. Grenet, Physica B: Condensed Matter **355**, 370 (2005).

[46]D. I. Novita, P. Boolchand, M. Malki, and M. Micoulaut, Journal of Physics: Condensed Matter **21**, 205106 (2009).

[47]L. C. Thomas, American Laboratory **33**, 26 (2001).

[48]S. Ravindren, K. Gunasekera, Z. Tucker, A. Diebold, P. Boolchand, and M. Micoulaut, The Journal of chemical physics **140**, 134501 (2014).

[49]K. Gunasekera, S. Bhosle, P. Boolchand, and M. Micoulaut, The Journal of chemical physics **139**, 164511 (2013).

[50]C. A. Angell, "Glass formation and the nature of the glass transitions," in *Insulating and Semiconducting Glasses*, edited by P. Boolchand (World Scientific, Singapore; River Edge, NJ, 2000) pp. 1–51.

[51]D. G. Georgiev, P. Boolchand, H. Eckert, M. Micoulaut, and K. Jackson, Europhysics Letters **62**, 49 (2003).

[52]L. C. Thomas, TA Instruments Technical Paper TP 006 (2005).

[53]E. Verdonck, K. Schaap, and L. C. Thomas, International journal of pharmaceutics **192**, 3 (1999).

[54]R. Brüning, E. Irving, and G. LeBlanc, Journal of Applied Physics **89**, 3215 (2001).

[55]M. Micoulaut and G. G. Naumis, EPL (Europhysics Letters) **47**, 568 (1999).

[56]M. Jin, P. Boolchand, and M. Mitkova, Journal of Non-Crystalline Solids **354**, 2719 (2008).

[57]V. V. Poborchii, A. V. Kolobov, and K. Tanaka, Applied Physics Letters **72**, 1167 (1998).

[58]S. Ravindren, K. Gunasekera, Z. Tucker, A. Diebold, P. Boolchand, and M. Micoulaut, Journal of Chemical Physics **140** (2014).

[59]K. Gunasekera, S. Bhosle, P. Boolchand, and M. Micoulaut, The Journal of Chemical Physics **139**, 164511 (2013).

[60]S. Yannopoulos and K. Andrikopoulos, Physical Review B **69**, 144206 (2004).

[61]G. Briegleb, Chem. Abt. A **144**, 321 (1929).

[62]R. Zallen and G. Lucovsky, "The interaction with light of phonons in selenium," in *Selenium*, edited by R. Zhigaro and W. C. Cooper (Van Nostrand Reinhold Company, New York, 1974) pp. 148–173.

[63]G. Lucovsky, in *The Physics of Selenium and Tellurium* (Springer, 1979) pp. 178–192.

[64]X. Feng, W. J. Bresser, and P. Boolchand, Phys. Rev. Lett. **78**, 4422 (1997).

[65]P. Chen, P. Boolchand, and D. Georgiev, Journal of Physics: Condensed Matter **22**, 065104 (2010).

[66]R. M. Martin, G. Lucovsky, and K. Helliwell, Physical Review B **13**, 1383 (1976).

[67]P. Boolchand, K. Gunasekera, and S. Bhosle, Physica Status Solidi B-Basic Solid State Physics **249**, 2013 (2012).

[68]P. Boolchand, B. L. Robinson, and S. Jha, Phys. Rev. B **2**, 3463 (1970).

[69]A. Von Hippel, The Journal of Chemical Physics **16**, 372 (1948).

[70]P. Boolchand and P. Suranyi, Phys. Rev. B **7**, 57 (1973).

[71]C. S. Kim and P. Boolchand, Phys. Rev. B **19**, 3187 (1979).

[72]P. Boolchand, T. Henneberger, and J. Oberschmidt, Phys. Rev. Lett. **30**, 1292 (1973).

[73]P. Boolchand, Solid State Communications **12**, 753 (1973).

[74]T. Henneberger and P. Boolchand, Solid State Communications **13**, 1619 (1973).

[75]P. Boolchand, T. Henneberger, and J. Oberschmidt, Physical Review Letters **30**, 1292 (1973).

[76]K. Jackson, A. Briley, S. Grossman, D. V. Porezag, and M. R. Pederson, Physical Review B **60**, R14985 (1999).

[77]J. Griffiths, G. Espinosa, J. Remeika, and J. Phillips, Physical Review B **25**, 1272 (1982).

[78]P. Boolchand, J. Grothaus, W. Bresser, and P. Suranyi, Physical Review B **25**, 2975 (1982).

[79]P. Boolchand, J. Grothaus, and J. Phillips, Solid State Communications **45**, 183 (1983).

[80]P. S. Salmon and I. Petri, Journal of Physics: Condensed Matter **15**, S1509 (2003).

[81]M. Micoulaut, A. Kachmar, M. Bauchy, S. Le Roux, C. Massobrio, and M. Boero, Physical Review B **88**, 054203 (2013).

[82]M. Durandurdu and D. Drabold, Physical Review B **65**, 104208 (2002).

[83]C. Massobrio, A. Pasquarello, and R. Car, Physical review letters **80**, 2342 (1998).

[84]R. Keezer and M. Bailey, Materials Research Bulletin **2**, 185 (1967).

[85]P. Boolchand, X. Feng, and W. Bresser, Journal of Non-Crystalline Solids **293**, 348 (2001).

[86]H. He and M. Thorpe, Physical Review Letters **54**, 2107 (1985).

[87]P. Boolchand, W. Bresser, M. Zhang, Y. Wu, J. Wells, and R. Enzweiler, Journal of non-crystalline solids **182**, 143 (1995).

[88]P. Boolchand and W. Bresser, Philosophical Magazine B **80**, 1757 (2000).

[89]K. Nakamura and A. Ikawa, Phys. Rev. B **66**, 024306 (2002).

[90]P. Lucas, A. Doraiswamy, and E. A. King, Journal of non-crystalline solids **332**, 35 (2003).

[91]J. Saiter, Journal of Optoelectronics and Advanced Materials **3**, 685 (2001).

[92]S. Chakraborty and P. Boolchand, The Journal of Physical Chemistry B **118**, 2249 (2014).

[93]W. Bresser, P. Boolchand, P. Suranyi, and J. de Neufville, Le Journal de Physique Colloques **42**, C4 (1981).

[94]W. Bresser, P. Boolchand, and P. Suranyi, Physical review letters **56**, 2493 (1986).

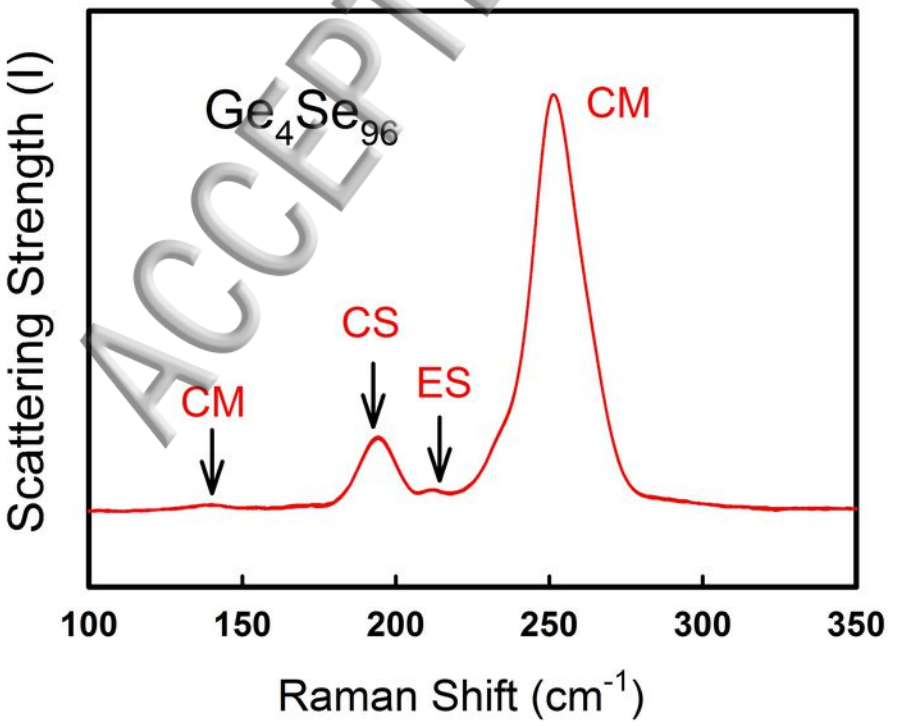
Ge4Se96
CM
CS
ES
CM
Scattering Strength (I)
100
150
200
250
300
350
Raman Shift (cm-1)

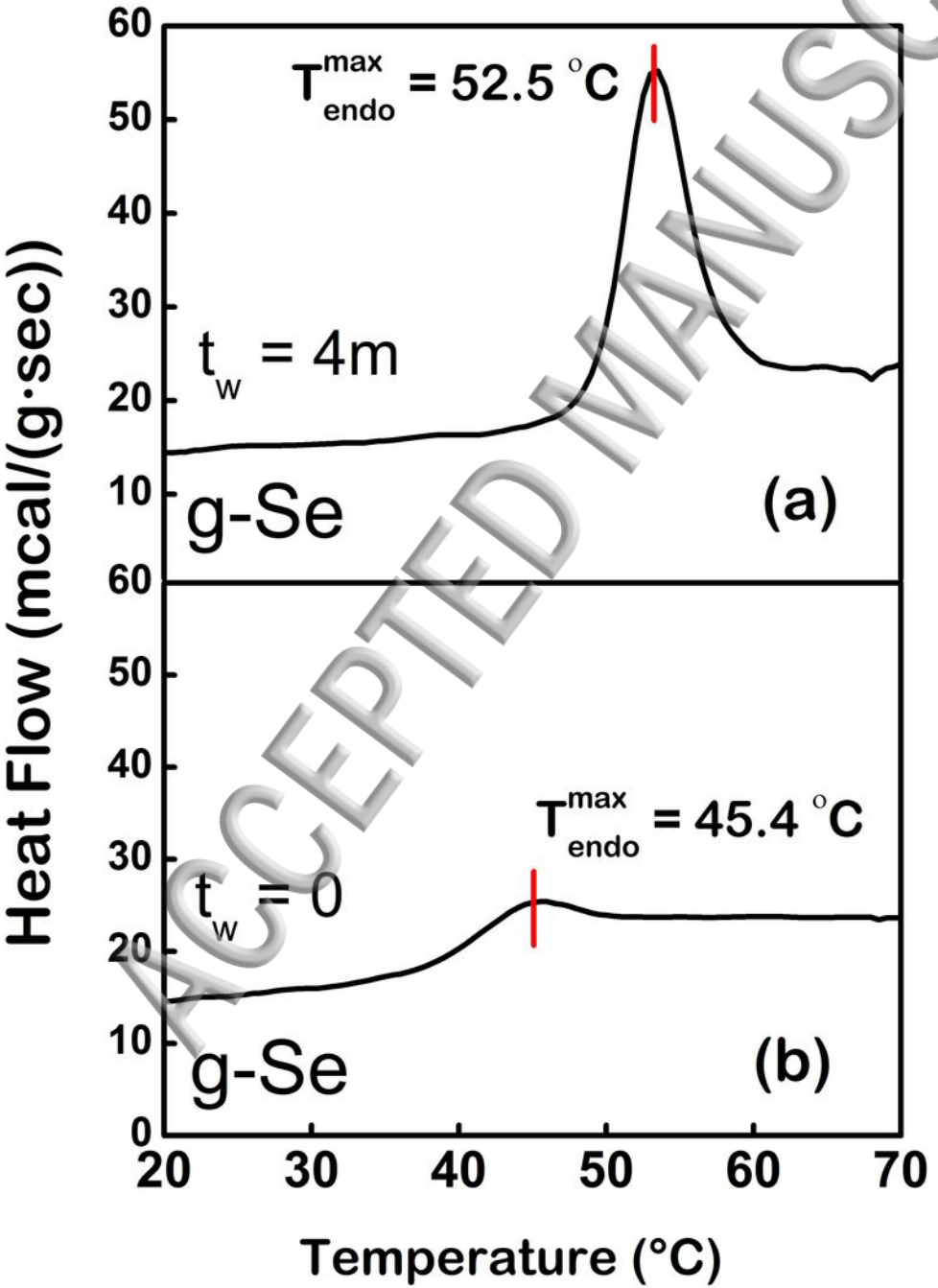

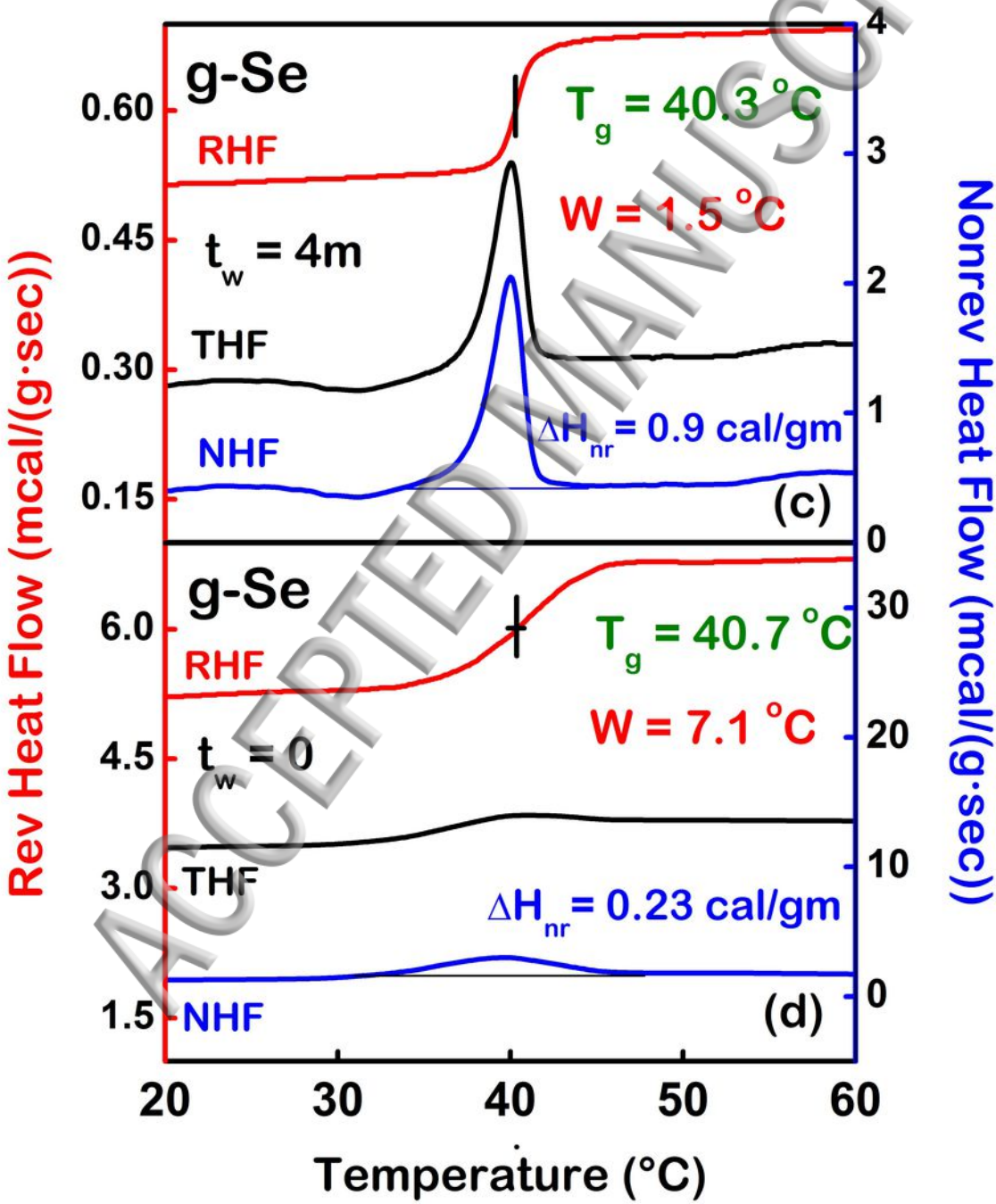

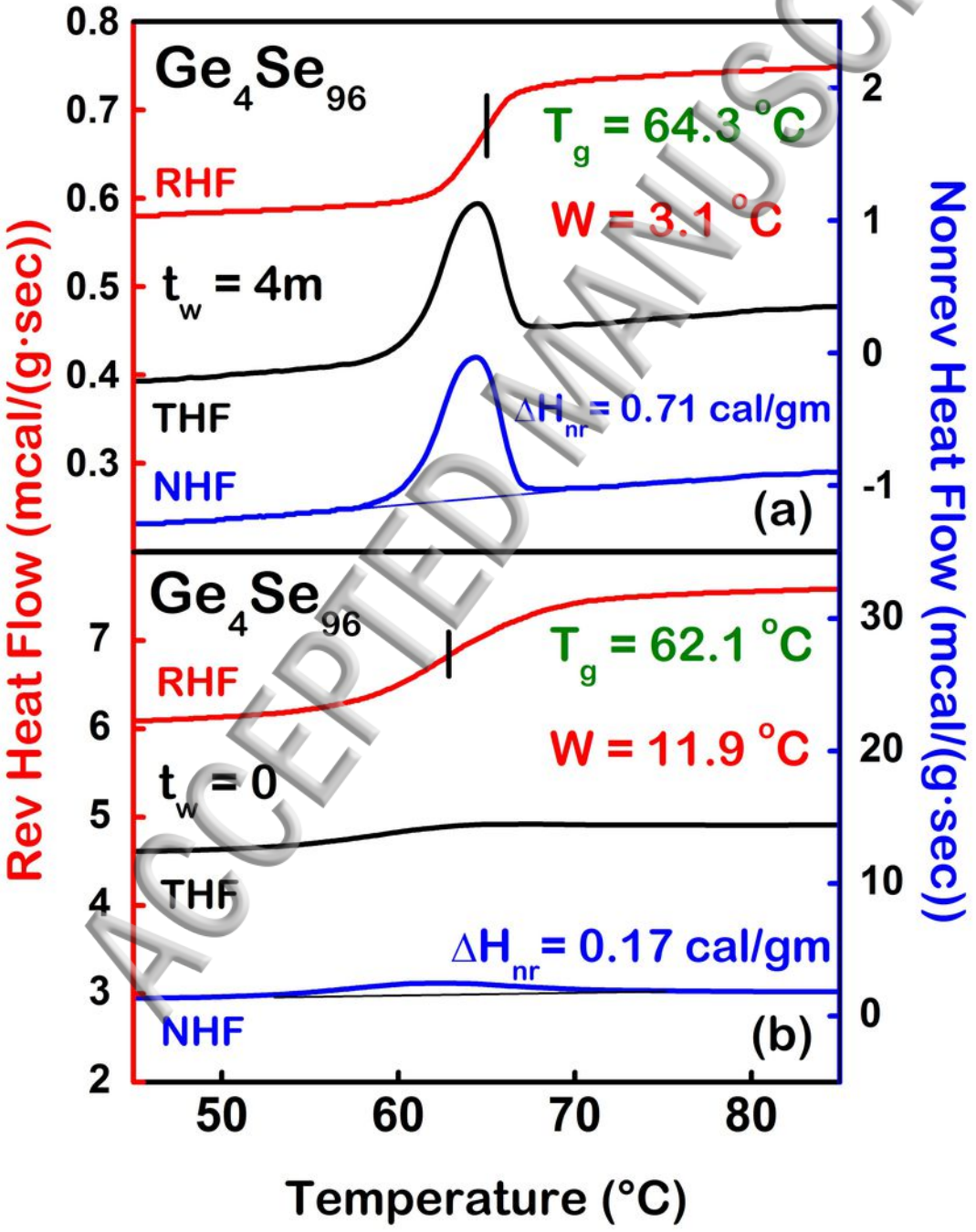

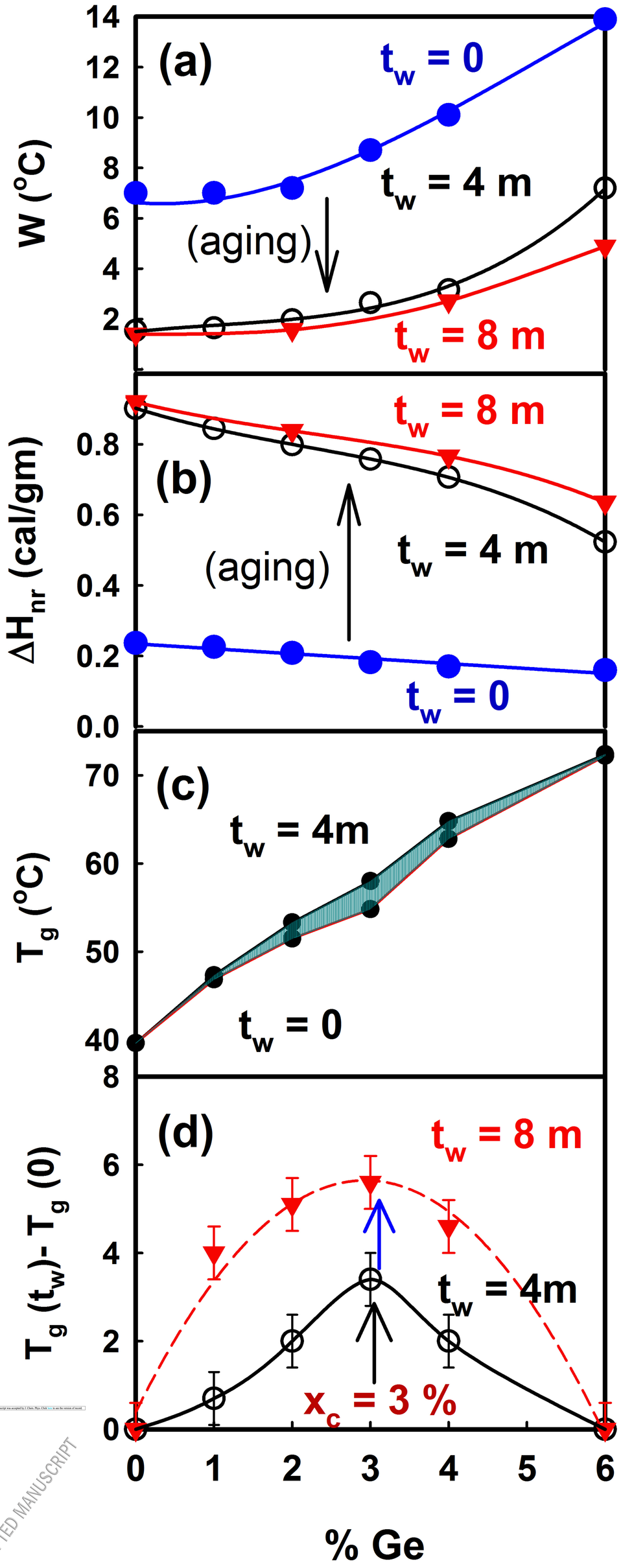

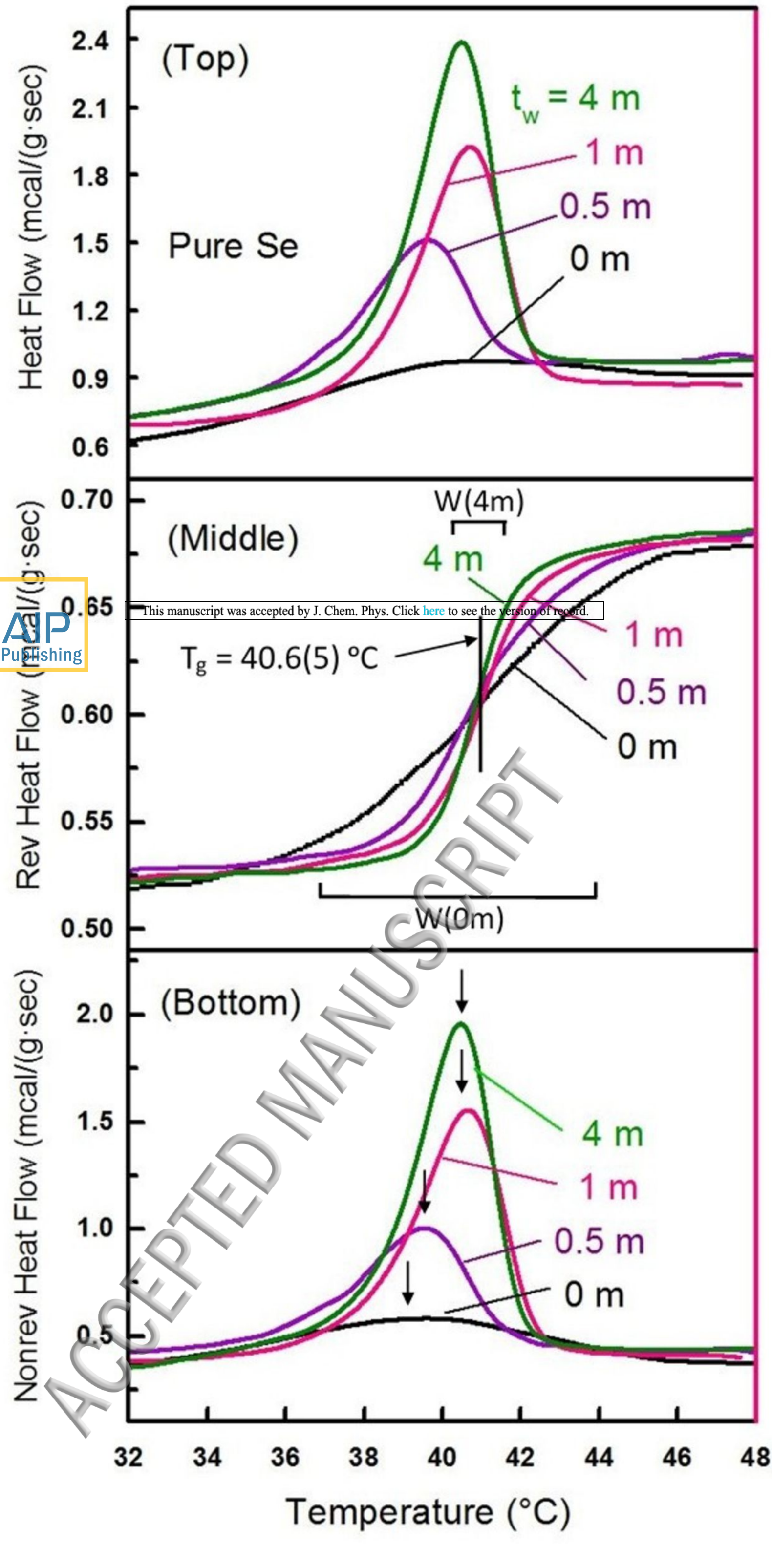

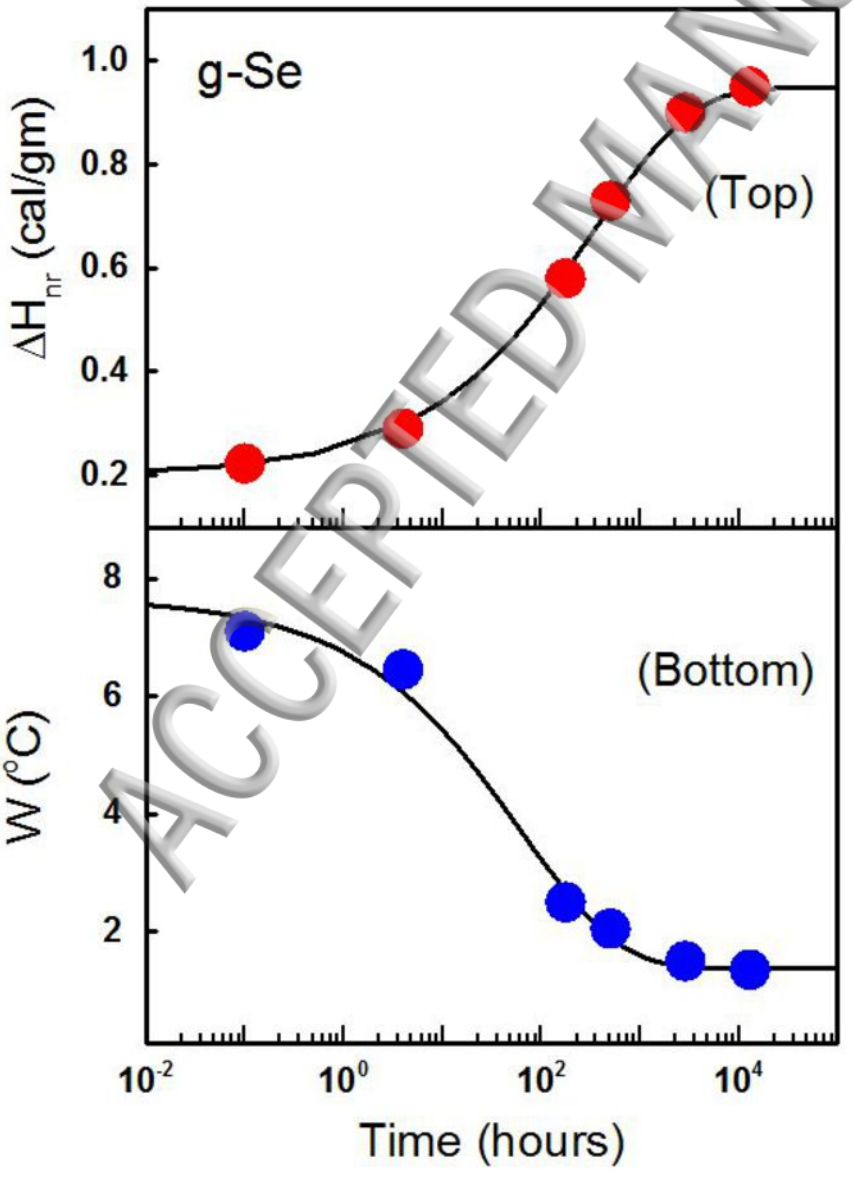

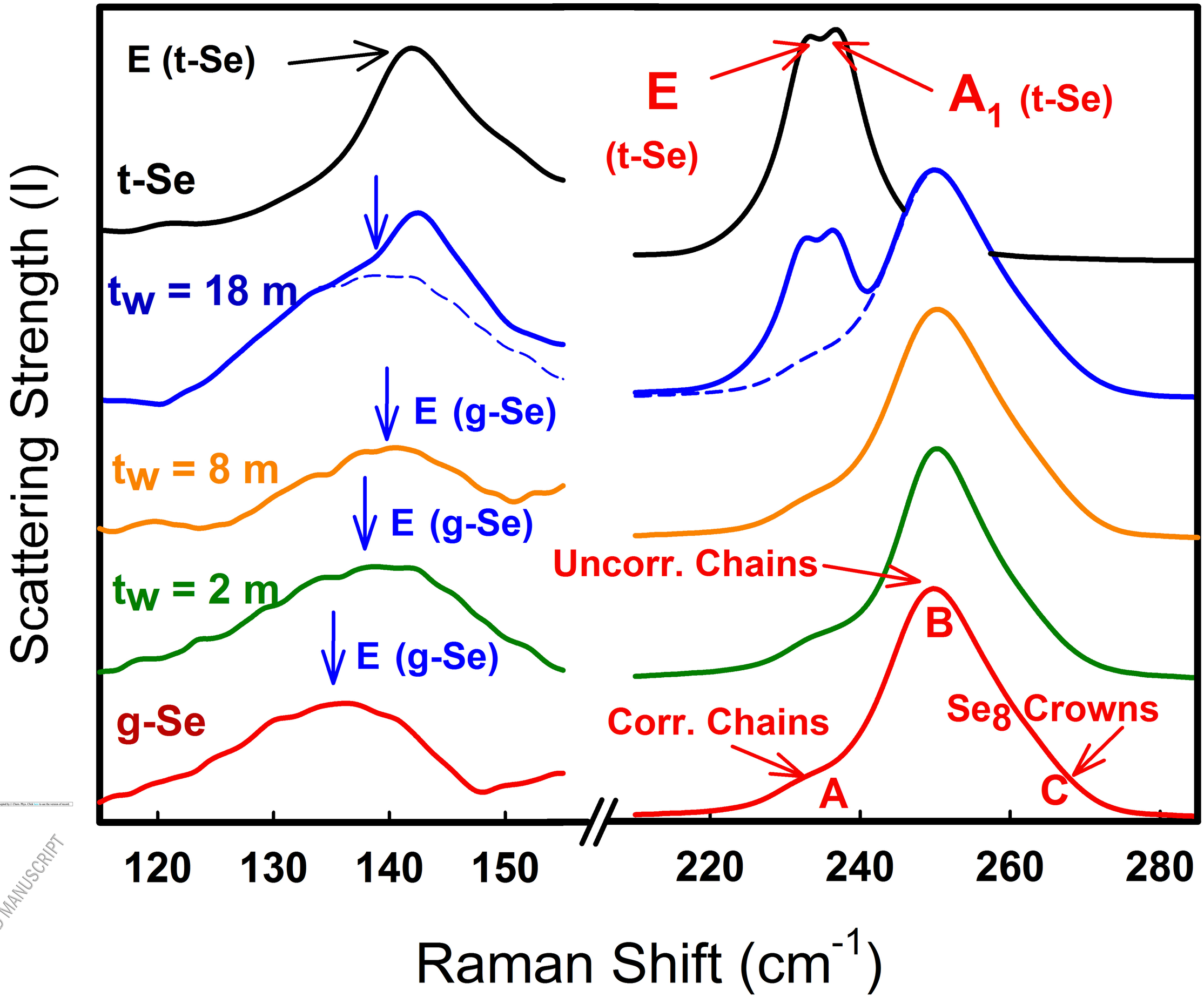

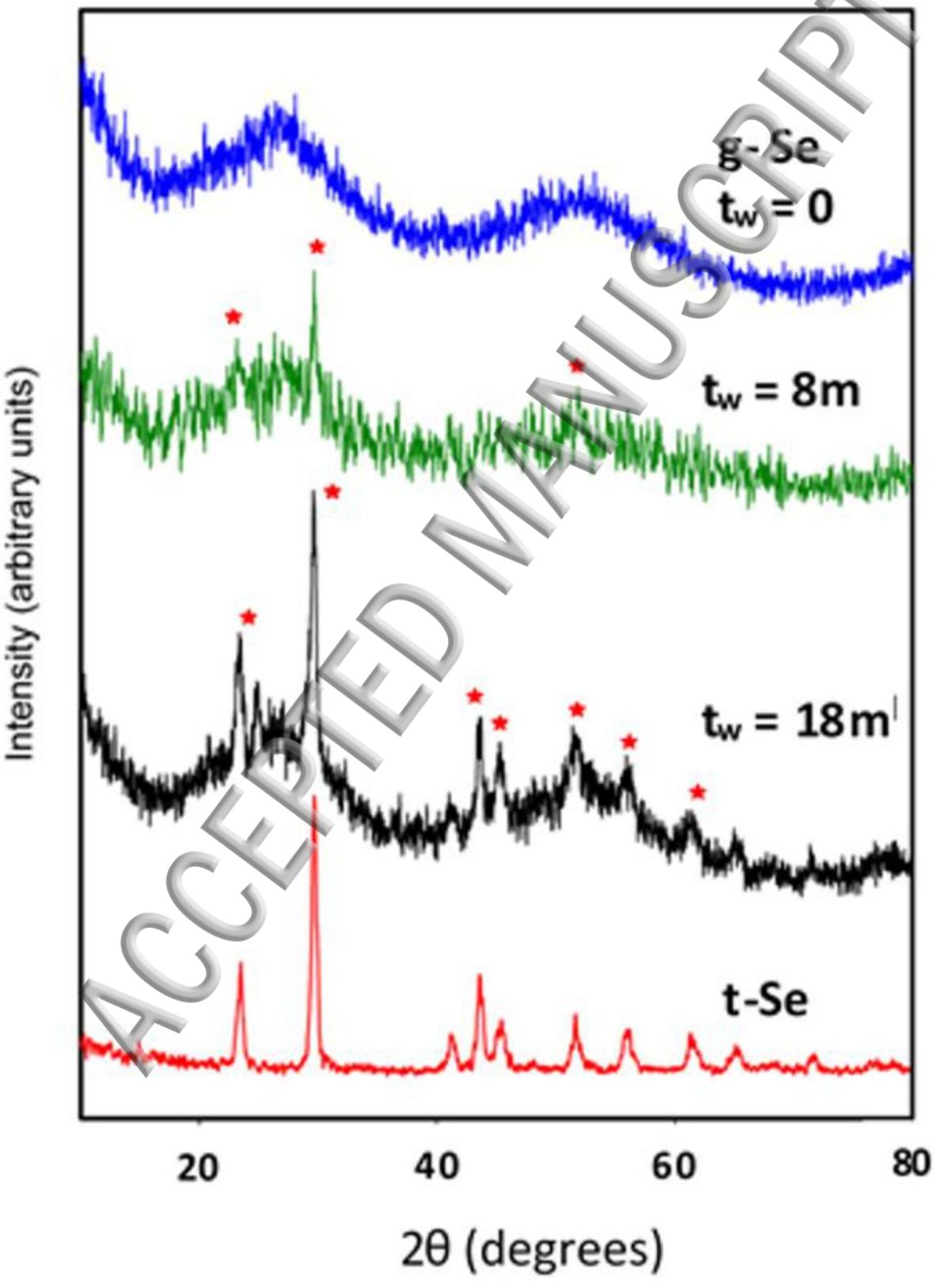

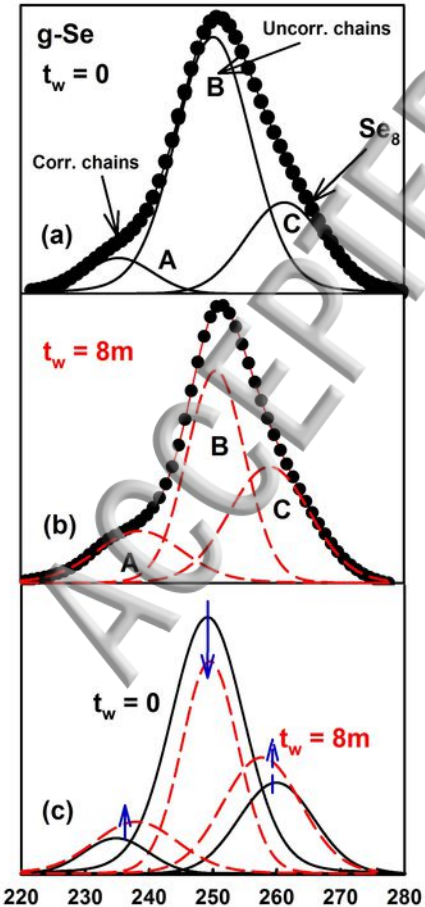
g-Se
t_w = 0
Uncorr. chains
B
Se_8
Corr. chains
(a)
C
A
t_w = 8m
B
C
(b)
A
t_w = 0
t_w = 8m
(c)
220
230
240
250
260
270
280
Raman Shift (cm^{-1})

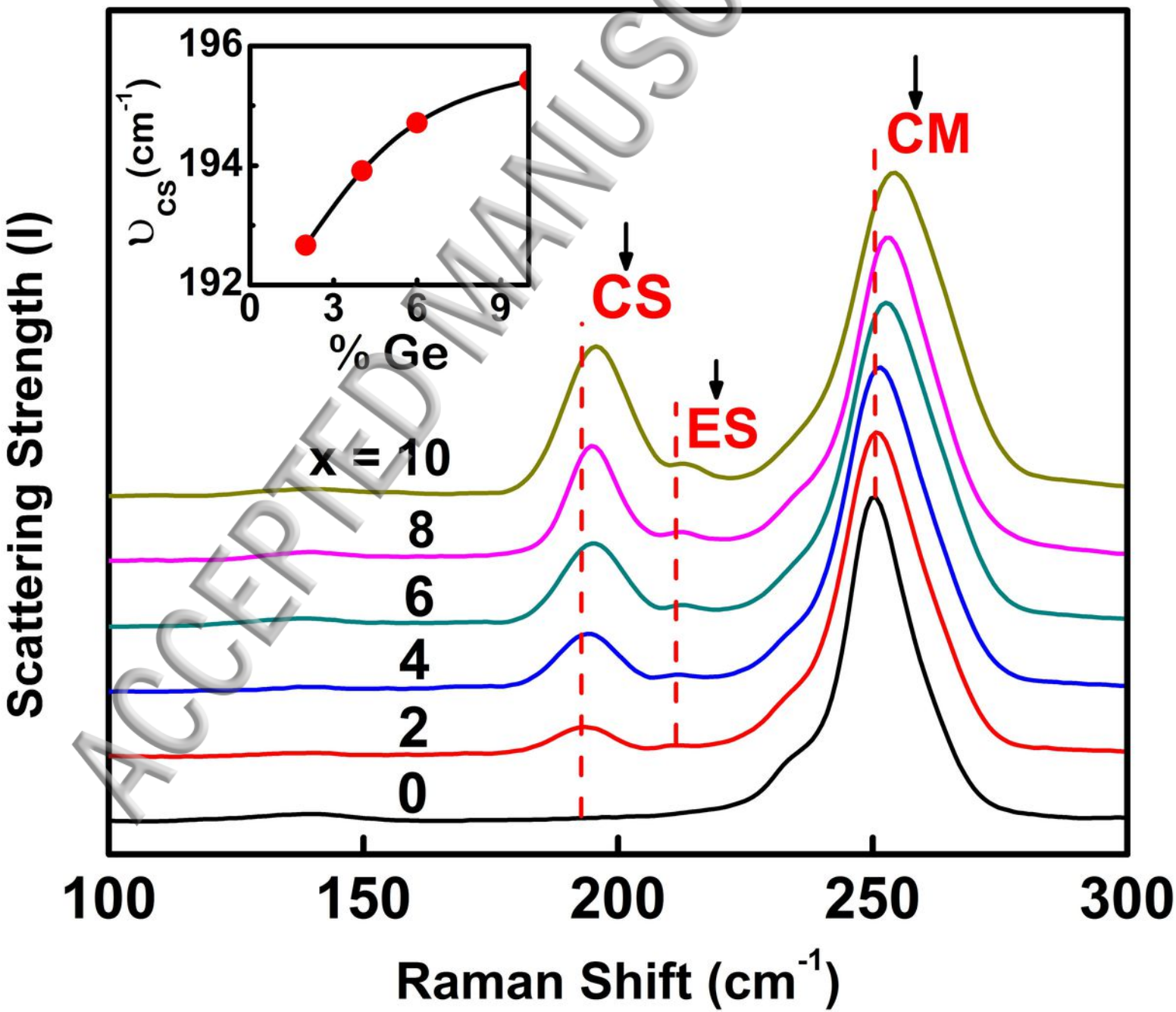

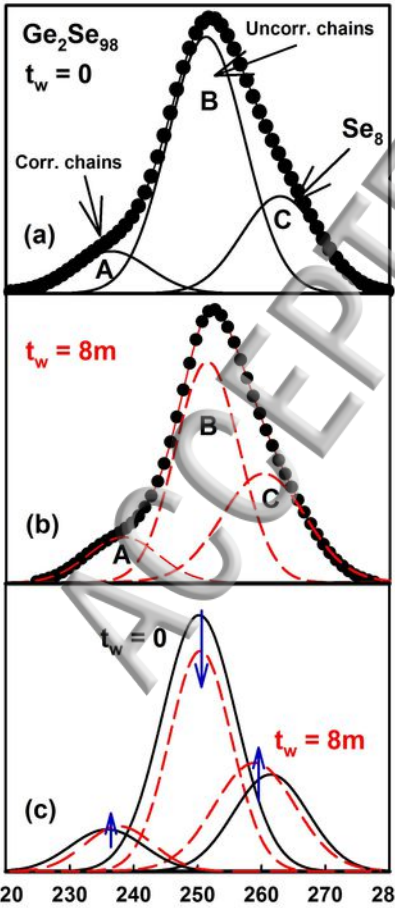
Ge2Se98
tw = 0
Uncorr. chains
B
Se8
Corr. chains
(a)
C
A
tw = 8m
B
C
(b)
A
tw = 0
tw = 8m
(c)
220
230
240
250
260
270
280
Raman Shift (cm-1)

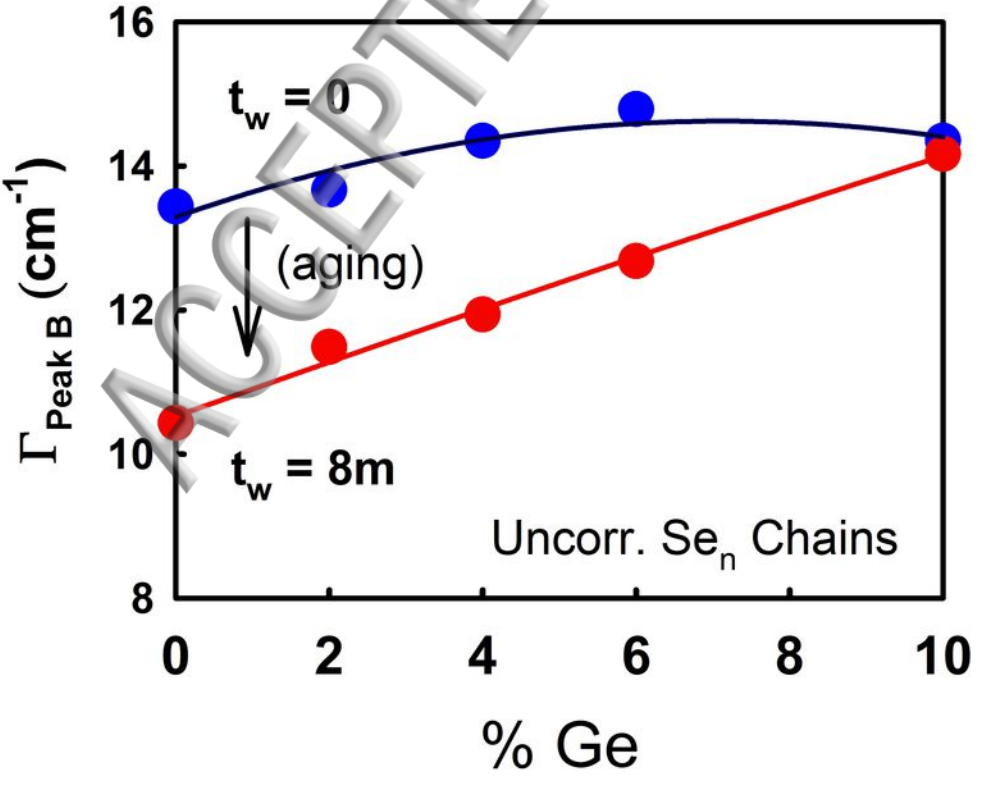
16
14
12
10
8
$\Gamma_{Peak\ B}$ (cm^{-1})
t_w = 0
(aging)
t_w = 8m
Uncorr. Se_n Chains
0
2
4
6
8
10
% Ge